MACHINE LEARNING & DATA ANALYTICS

FRIEDRICH-ALEXANDER UNIVERSITÄT ERLANGEN-NÜRNBERG
TECHNISCHE FAKULTÄT

Assessment of Cold Face Test for Stress Reduction

Bachelor's Thesis in Medical Engineering

submitted
by

Janis Joshua Zenkner

born 29.06.1997 in Schwäbisch Hall

Written at

Machine Learning and Data Analytics Lab (CS 14)
Department of Computer Science
Friedrich-Alexander-Universität Erlangen-Nürnberg (FAU)

Advisors:
Robert Richer, M.Sc., Arne Küderle, M.Sc., Prof. Dr. Bjoern Eskofier
(*Machine Learning and Data Analytics Lab, FAU Erlangen-Nürnberg)*,
Prof. Dr. Nicolas Rohleder
(*Chair of Health Psychology, FAU Erlangen-Nürnberg)*

Started: 15.06.2019

Finished: 14.12.2019

Ich versichere, dass ich die Arbeit ohne fremde Hilfe und ohne Benutzung anderer als der angegebenen Quellen angefertigt habe und dass die Arbeit in gleicher oder ähnlicher Form noch keiner anderen Prüfungsbehörde vorgelegen hat und von dieser als Teil einer Prüfungsleistung angenommen wurde. Alle Ausführungen, die wörtlich oder sinngemäß übernommen wurden, sind als solche gekennzeichnet.

Die Richtlinien des Lehrstuhls für Bachelor- und Masterarbeiten habe ich gelesen und anerkannt, insbesondere die Regelung des Nutzungsrechts.

Erlangen, den 16.12.2019

Übersicht

Von Stress verursachte oder begünstigte Krankheiten zählen zu den am häufigsten auftretenden chronischen Krankheiten. Jedoch behandeln die meisten Stressinterventionsmethoden lediglich die Symptome von Stress. Daher werden Methoden, die das Stresssystem vor der Deregulation bewahren, dringend benötigt. Die Hypothalamus-Hypophysen-Nebennierenrinden (HPA) Achse und der sympathische Zweig des autonome Nervensystem (ANS) kontrollieren die Erzeugung der Stressantwort. Vom Vagusnerv, einem der Hauptnerven des parasympathischen Zweigs des ANS - und damit Antagonist des sympathischen Zweigs, wird hingegen angenommen, dass er einen hemmenden Effekt auf die HPA-Achse hat. Daher soll im Rahmen dieser Arbeit der Effekt parasympathtischer Stimulation auf die Stresserzeugung untersucht werden. Genauer gesagt wird der Cold Face Test als alternative Maßnahme, den Tauchreflex auszulösen, verwendet, um die Stressantwort durch die induzierte parasympathische Aktivität zu inhibieren.
Hierfür wurden 28 Probanden in einer Interventions- und Kontrollgruppe einem standardisierten Stressprotokoll, dem Montreal Imaging Stress Task (MIST), ausgesetzt. Dabei wurde ein Elektrokardiogramm aufgenommen und Parameter wie Herzrate und Herzratenvariabilität abgeleitet. Zudem wurde Kortisol mittels Speichelproben erfasst. Zusammen mit den elektrophysiologischen Variablen wurde somit die Aktivität der HPA-Achse und des ANS erfasst.
Sowohl Kortisolkonzentration als auch Herzrate zeigten einen deutlichen Anstieg als Reaktion auf den MIST. Im Gegensatz zur Kontrollgruppe, die am höchsten Wert nach Durchführung der Stressaufgabe einen Kortisolanstieg von 42.89% im Vergleich zum Ausgangswert zeigte, sanken die Kortisolwerte der Intervenstionsgruppe im Mittel sogar um 14.42%. Tatsächlich zeigte die Interventionsgruppe signifikant niedrigere Kortisolwerte und -ausschüttung. Zudem wies die Kontrollgruppe signifikant ansteigende Herzraten in den Ruheintervallen während der Stressaufgabe auf, wohingegen die Ruheherzraten der Interventionsgruppe im Verlauf der Stresstudie konstant blieben. Diese Ergebnisse lassen vermuten, dass die Durchführung des Cold Face Tests vor dem Auftreten des Stressors mit einer reduzierten Kortisolausschüttung und einer schnelleren Rückkehr zu den Ausgangswerten einhergeht und somit die Erzeugung der Stressantwort hemmt.
Der in dieser Arbeit vorgestellte Ansatz, den Cold Face Test als aktive Stressinterventionsmaßnahme zu verwenden, könnte in weiteren Arbeiten hinsichtlich therapeutischer Gesichtspunkte bzw. möglicher Langzeiteffekte auf deregulierte Stresssysteme weiter erforscht werden.

Abstract

Stress-related diseases count to the most often occurring chronic diseases. However, most of the present stress intervention methods actually just cope with the symptoms of stress. Hence, the need for methods that prevent the stress system from deregulation is steadily increasing. The Hypothalamus-Pituitary-Adrenal (HPA) axis and the Autonomous Nervous System (ANS) control the creation of the human stress response. The vagus nerve, a major nerve of the parasympathetic branch of the ANS, is assumed to possess an inhibitory effect on the HPA axis. Therefore, this work introduces the Cold Face Test, a measure to induce vagal stimulation by triggering the Diving Reflex, as a method to inhibit the stress response creation on a biological level.

28 healthy subjects were exposed to a standardized test protocol, the Montreal Imaging Stress Task. Derived from the electrocardiogram, the heart rate and heart rate variability were computed. Along with the electrophysiological features, cortisol levels obtained from the saliva samples and cortisol-derived features were used to assess the activation of the HPA axis and of the ANS.

The Control group showed a mean cortisol increase of 42.89% at the peak level compared to the initial concentration. In contrast, the Intervention group showed a decrease of 14.52% at the cortisol peak after the stress task. In fact, significantly lower cortisol levels and stress-induced cortisol secretion was shown in the Intervention group. Moreover, the Intervention group showed a constant baseline heart rate, whilst the baseline of the Control group showed significant increases between the single stress tasks. The results indicate that the conduction of the Cold Face Test prior to a stressor is associated with reduced cortisol increase and faster recovery. Thus, it effectively inhibits the stress response creation.

In further work, effects of the Cold Face Test with a therapeutic focus on deregulated stress systems or long-term stress reducing effects could be assessed.

Contents

1 Introduction **1**

2 Medical Background **5**

2.1 Stress System 5

2.1.1 Autonomous Nervous System 6

2.1.2 Hypothalamus-Pituitary-Adrenal axis 7

2.1.3 Heart Rate Variability 8

2.2 Diving Response 9

3 Related Work **13**

3.1 Acute Stress Induction 13

3.2 Stress Reduction and Biofeedback 14

3.3 Cold Face Test 16

4 Methods **19**

4.1 Cold Face Test 19

4.2 Data Acquisition 20

4.3 Data Processing 21

4.3.1 R-Peak Detection 22

4.3.2 CFT-specific features 23

4.3.3 RMSSD 24

4.3.4 RR50 / pNN50 24

4.3.5 Respiratory Sinus Arrhythmia 26

4.3.6 SD1 and SD2 26

4.3.7 Cortisol-derived features 28

5 Evaluation **31**
5.1 Montreal Imaging Stress Task 31
5.2 Study Design 33
5.3 Measures 36

6 Results **39**
6.1 MIST Responses 39
6.1.1 Electrophysiological Measures 39
6.1.2 Mood 41
6.2 Responses to the Cold Face Test 42
6.3 Distinction between Cold Face Test and Control group 43
6.3.1 Electrophysiological Measures 43
6.3.2 Cortisol 46
6.3.3 Mood 48
6.3.4 Differences in Cold Face Test Responder Types 49

7 Discussion **51**
7.1 Responses to the Stress Task 52
7.2 Responses to the Cold Face Test 52
7.3 Distinction between Cold Face Test and Control Group 53
7.3.1 Electrophysiological Measures 53
7.3.2 Cortisol 54
7.3.3 Mood 55
7.4 Distinction between Responder Types and Control 55

8 Conclusion and Outlook **57**

A Patents **59**

B Additional Figures and Tables **61**

Glossary **65**

List of Figures **67**

List of Tables **69**

Bibliography **70**

Chapter 1

Introduction

The Health and Safety Executive in the United Kingdom states that in 2018/19 stress-related diseases accounted for 12.8 billion days, i.e. 54% of all working days lost due to ill health, amounting to an economical loss of more than 12$ billion [Hea].
In spite of the wide-spread opinion that stress is generally "bad", it is actually crucial to survival. Strong endocrinological and neural reactions result from stress and thus set the human body into an alert state enabling to rapidly adapt to new situations. This response is initiated by the activation of the *Sympathetic Nervous System (SNS)*, one of the two major components of the *Autonomous Nervous System (ANS)*. The *SNS* induces the arousing "fight or flight" reaction, hence causing an increase in heart rate, dilatation of the pupils and enhanced blood flow to the skeletal muscles and lungs. In contrast, the *Parasympathetic Nervous System (PSNS)* is responsible for the relaxing "rest and digest" reaction of the human body manifested in a decrease in heart rate, enhanced saliva secretion and the dilatation of blood vessels leading to the gastro-intestinal tract [Lan07]. For this reasons, both parts of the *ANS* play an important role in the creation and control of the human stress reaction. Another major stress pathway is the *Hypothalamus-Pituitary-Adrenal (HPA)* axis that regulates the creation of the human stress response. The *HPA* axis is responsible for the secretion of cortisol, whilst the *ANS* induces, among other effects, the secretion of adrenaline [Dun07]. Both hormones count to the most important stress markers [Lan07].
However, stress is not caused by one single aspect. In contrary, it is a multi-faceted process that is influenced by a multitude of biological as well as environmental factors, such as, for instance, socioeconomic status or political situation [Ame17]. Due to the perceived growing unsteadiness in politics and economics, stress or the perception of stress increases nowadays [Ame17].
There are two types of stress: acute stress and chronic stress. Acute stress induces the physical adaption to changing environmental factors and thus poses an essential process. In contrast,

chronic stress compromises the occurrence of stressors with a high frequency and hence the accumulation of minor, day-to-day stresses [McE98]. Yet, the repeated and cumulative exposure to acute stress (with a lower rate) also leads to a frequently activated stress system. Thus, the repeated adaption to an uncertain environment in the face of acute stress also goes in hand with costs, i.e. the allostatic load, that contribute to the negative impact of chronic stress. Despite the essential aspects of acute stress, it is one basic element in the dysregulation of the stress system [McE00].

There are various psychological and physiological comorbidities such as cardiovascular diseases and adverse reactions on the metabolism that result from the dysregulation of the stress system. Moreover, stress may cause − or at least promote − various other disorders, for instance, depression and anxiety. Both count to the most often occurring chronic diseases [Fol10]. Along with the previously mentioned increasing stress perception and the economical and healthcare costs relating thereto, the need for methods that prevent a deregulated stress system is gaining in importance.

While methods that serve the stress reduction exist, they, however typically, deal with the symptoms of stress. Conversely, there is a lack of methods that actually biologically prevent the stress system from deregulation caused by acute stress. Since there are links between the *ANS* and the *HPA* axis through the hypothalamus and the amygdala, a stimulation of the *PSNS* before an acute stressor may lead to a reduced stress response.

So far, many researches focused on the reduction of stress related symptoms or relaxation-based approaches to cope with stress. However, only little research is present in the field of the biological interference with the stress system and acute stress that exploits the link between *ANS* and *HPA* axis, despite the knowledge about the stress system and the costs that go along with stress-related diseases.

A mean that may make use of this link is presented by the *Diving Response (DR)* (also referred to as “Diving Reflex”) - a mechanism that is triggered by the facial immersion in water and contributes to the conservation of oxygen. The *Cold Face Test (CFT)* poses an alternative approach to trigger the *DR* also inducing parasympathetic activity. This *CFT*-induced activity of the *PSNS* is assumed to interfere with the stress system [Khu07]. Consequently, the application of the *CFT* prior to exposure to acute stress is hypothesized to interfere with the stress response creation. Thus, this thesis investigates the suitability of the *CFT* as a measure to inhibit the acute stress response creation.

The thesis is structured as follows: After introducing the medical background necessary for understanding the biological mechanisms: the function of the *ANS*, the *HPA* axis, and the *DR* in

Chapter 2, a comprehensive review of literature and previous work related to the *CFT*, biofeedback for stress reduction and acute stress induction by means of the *Montreal Imaging Stress Task (MIST)* is given in Chapter 3. Subsequently, the data acquisition and processing is outlined in Chapter 4. In Chapter 5, the evaluation of the proposed approach is explained, together with a presentation of results and discussion in Chapters 6 and 7, respectively. Finally, the thesis is concluded in Chapter 8 along with an outlook on how further research can built upon this work.

Chapter 2

Medical Background

In this chapter, the underlying medical mechanisms necessary for this thesis are introduced and explained in more detail: Firstly, the stress system is described, focusing on the *ANS* and *HPA* axis, followed by a section on the Diving Response and Cold Face Test, respectively.

2.1 Stress System

Stress can be divided into *acute* and *chronic* stress. Situations leading to acute stress, such as job interviews or exams, are usually elicited by novelty, uncertainty or the assumption of threat. However, there is no generally accepted definition of psychological stress and its triggers. Nonetheless, the feeling of threat certainly poses a core element in the elicitation of stress [Tha12]. Once exposed to a so-called *stressor*, the human body initiates a response consisting of a wide variety of physiological mechanisms ranging from increased heart rate, dilated pupils and a widened thorax to sweaty hands [Khu07]. Subsequently, those stress-induced reactions are referred to as the *stress response*.

Even though stress is in general negatively connoted, it is crucial to surviving. The stress response, on the one hand, prepares for a potential upcoming event. Therefore, stress is accompanied by an evolutionary advantage, since the increased alertness after rustling in a close bush might be essential if the noise is caused by a dangerous animal [Cha05]. On the other hand, this reaction constitutes a negatively biased behavior since each unexpected situation is assumed to pose a potential threat [Cac99]. Apparently, if malfunctioning, this mechanism generates adverse reactions resulting in physiological and psychological constraints [Khu06].

As complex as the generation of the human stress response is, it can be narrowed down to two players that govern the stress response creation: the Hypothalamus-Pituitary-Adrenal (*HPA*) axis and the Sympathetic Nervous System (*SNS*) as a part of the Autonomous Nervous System (*ANS*). Both taken together yield in the human stress system (Figure 2.1) [Cha05].

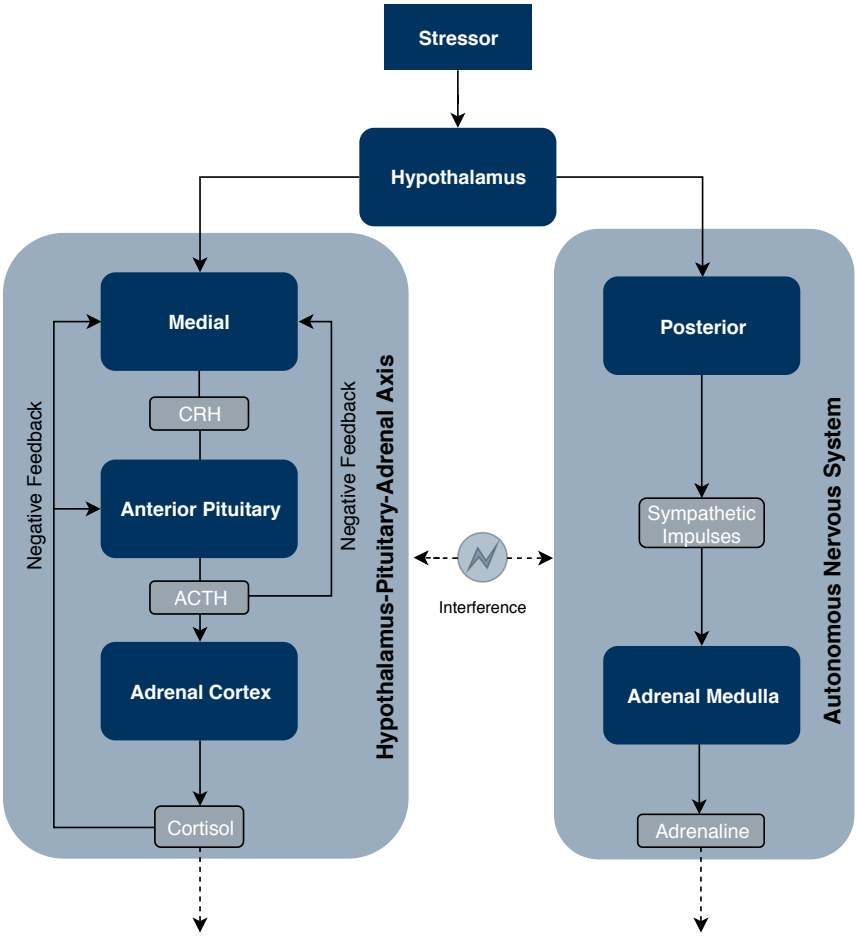

Figure 2.1: Schematic illustration of the stress system. The stress response is generated by *HPA* axis (left) and *ANS* (right).

2.1.1 Autonomous Nervous System

The *ANS* splits into the *PSNS* and its antagonist, the *SNS*. In general, parasympathetic activity inhibits processes that are moderated by the *SNS* and vice versa. Whereas the *PSNS* is mainly responsible for the 'rest-and-digest' response, the *SNS* governs the 'fight-and-flight' response. Therefore, sympathetic activity dominates the actions of the *ANS* during stress exposure [Cha05].

The *SNS* originates from the posterior hypothalamus. Once exposed to a stressor, the hypothalamus is stimulated by the limbic system, which is, among other functions, responsible for processing emotions and behavior [Rai07]. Therefore, sympathetic impulses are transmitted to the heart and adrenal glands. As a result, the adrenal medulla secretes the hormone adrenaline [Fol10].
Besides the endocrinological effects, the *ANS* controls the heart and cardiac system in general [Fol10]. More precisely, the heart rhythm is regulated by the sinus node which, in turn, is controlled by the *ANS*. Therefore, the *Heart Rate (HR) increases* during times of increased *sympathetic* activity and *decreases* during times of increased *parasympathetic* activity. Due to the parasympathetic and sympathetic interference with the cardiac system, the *HR* varies even during resting periods or periods with constant physical and psychological load [Ber97].
Furthermore, the *ANS* intervenes the acinar cells that primarily produce the components of saliva [Nat09]. Therefore, an activation of the different parts of the *ANS* results in differences in the endocrinological composition of saliva and an altered secretion rate. Sympathetic activation results, for instance, in a dry mouth, increased salivary cortisol and alpha amylase levels, among others. Therefore, the salivary concentration of both cortisol and amylase are indirect indicators for (acute) stress. Whereas cortisol promotes the generation of sugar in the liver, alpha amylase catalyzes the cleavage of starch into sugar. Thus, both hormones enhance the energy supply [Nat09].
As shown in Figure 2.1, the *ANS* interacts with the *HPA* axis [Tha06b]. In fact, the *ANS* is assumed to possess a regulatory effect on the *HPA* axis [Tha06a]. According to [Tha06b], especially the vagus nerve, a major nerve of the *PSNS*, inhibits the *HPA* axis. Moreover, the cardiac nerves come off the vagus nerve. Therefore, the *PSNS* is assumed to be part in a negative feedback system that inhibits the cortisol output and the cardiac system. Thus, the vagus nerve is assumed the be an inhibitor of the stress system [Mar11].

2.1.2 Hypothalamus-Pituitary-Adrenal axis

Similar to the *ANS*, the *HPA* axis is controlled by the hypothalamus and modulated by the limbic system. If one is exposed to a stressor, the medial hypothalamus secretes the peptide *Corticotrophin-Releasing Hormone (CRH)* that consequently migrates to the pituitary gland where *Adrenocorticotropic Hormone (ACTH)* is released. As a result of the increased *ACTH* concentration, *cortisol* is secreted by the adrenal cortex [Orb13]. The released cortisol enters a negative feedback cycle that inhibits the *ACTH* output of the pituitary gland. Additionally, the *CRH* secretion is decreased by cortisol reducing the *ACTH* output even further [Cha05].

Elevated levels of glucocorticoids, such as cortisol, lead to improved fitness by mobilizing energy [Sch10]. Hence, increased cortisol concentrations prepare the human body for 'fight or flight' actions by inhibiting nonessential functions, such as the production of saliva, and enhancing essential ones, such as cardiac activity. Therefore, cortisol has been established as a reliable marker for the measurement of acute stress [Kir94]. Cortisol levels can be measured in the blood (serum cortisol) or in saliva (salivary cortisol). Due to less invasiveness and higher repeatability, acute (as well as chronic) stress levels are usually measured with salivary cortisol samples [Kir89]. In general, the cortisol concentration increases in response to acute stress, reaching the maximum level approximately 15 minutes after being exposed to the stressor. Within two hours, the concentration usually reaches its baseline again [Orb13].
As for most cases, the state of equilibrium is fragile. The malfunctioning of a single contribution might upset the balance of the whole system. This phenomenon applies for the cortisol feedback cycle as well as the whole stress system. An irregular cortisol regulation includes a lack of adaption to repeated stressors of the same type, a decelerated decrease of cortisol levels, as well as increasing hormone levels even after the stress ended [McE98]. Consequently, improper cortisol and adrenaline secretions can cause adverse reactions [DR03].

2.1.3 Heart Rate Variability

Heart Rate Variability (HRV) is defined as the ability of an organism to quickly adapt its heart rate to external stimuli [Sam14]. Morover, it represents a marker for the activity of the *ANS* and thus, for a possible malfunctioning of the stress system. Lately, it has become extremely popular in various biomedical research fields [Sgo15].
The term *HRV* actually contains various features computed from the course of heart rate that index the variance, rhythm, or complexity of successive heart beats, usually measured by variations of RR-Intervals [Sam14]. In other words, the *HRV* displays the interplay of sympathetic and parasympathetic nervous system [Sam14]. For this reason, a high *HRV* suggests that there is a lively interplay between both axes of the *ANS*. Hence, it is assumed to mirror the ability of an organism to rapidly adapt to changing environmental demands [Tha07].
In contrast, a system that is not able to adapt and break its specific pattern, even in times of struggle, is deregulated [Tha12]. Accordingly, various diseases are assumed to go in hand with decreased *HRV* ranging from disorders of the *ANS*, such as Parkinson's disease [Fre95], over psychological diseases, such as depression [Sgo15], to all-cause mortality [Tha12].
In addition to the autonomic regulation of the cardiac system, the *HR* is modulated by respiration. Over the course of one respiration cycle, the heart rate increases during expiration and decreases

during inspiration [Eck83][Kat75]. This depicts the cyclic waxing and waning of the vagal innervation of the sinus node [Gro90]. The *Respiratory Sinus Arrhythmia (RSA)* assess this process quantitatively. A decreased *RSA* displays the decoupling of respiration and cardiac rhythm and thus the decreased ability to adapt the heartbeat to changed respiratory requests [Gro07].
Along with respiration, numerous factors such as gender, age, cardiovascular diseases, and high temperatures affect the *HRV* [Zuc09][Tha06b]. Moreover, there is an increased *HRV* in athletic people due to the decreased resting *HR*. Typically, the *HRV* decreases during stressful phases due to predominating sympathetic activity. Here, stressful phases can either be caused by physical stress (i.e. physical activity) or psychological stress [Ber97].

2.2 Diving Response

The *DR* is a mechanism that is triggered by apnea as a response to the immersion in water. Thus, it is defined as a "characteristic pattern of respiratory, cardiac and vascular responses triggered by breath-hold diving" [Goo94]. However, it is sufficient to immerse the face in water. Previous work has shown that especially the stimulation of the eye and forehead region result in a strong response [Nel80]. These areas are supplied by two of the three branches of the the trigeminal nerve, i.e. the ophthalmic and maxillary branch (Figure 2.2a). Thus, the facial immersion in water results in the stimulation of the trigeminal nerve [Khu07].
Remarkably, the stimulation can also be achieved by the application of a cold stimulus to the face. However, so far it is not well understood why the cold stimulus induces the same stimulation as the facial immersion in water [Khu06].
Nevertheless, the stimulated trigeminal nerve transfers the elicitation to the brainstem as it is one of the twelve cranial nerves. Hence, the vagus nerve, the tenth cranial nerve that also originates from the brainstem, is also stimulated by the trigeminal elicitation (see Figure 2.2b). This series of reactions is called the *trigeminal-vagal reflex arc*. The vagus nerve is not only a cranial nerve, but one of the major nerves of the *PSNS*. Thus, the initial elicitation of the trigeminal nerve results, mediated by the vagus nerve, in the stimulation of the *PSNS*.
Triggered by the enhanced parasympathetic activity, the heart rate, as well as the blood flow to the limbs, slow down, whereas the mean arterial blood pressure is slowly increasing [Goo94]. Moreover, the cerebral vasoconstriction decreases, whereas the peripheral vasoconstriction increases resulting in an increased blood flow to the brain [Bro03]. Along with the reduction of heart rate and blood redistribution, numerous peripheral and central *DR*-induced physiological responses yield in a mechanism that saves oxygen. Hence, it prolongs the functionality of the vital organs

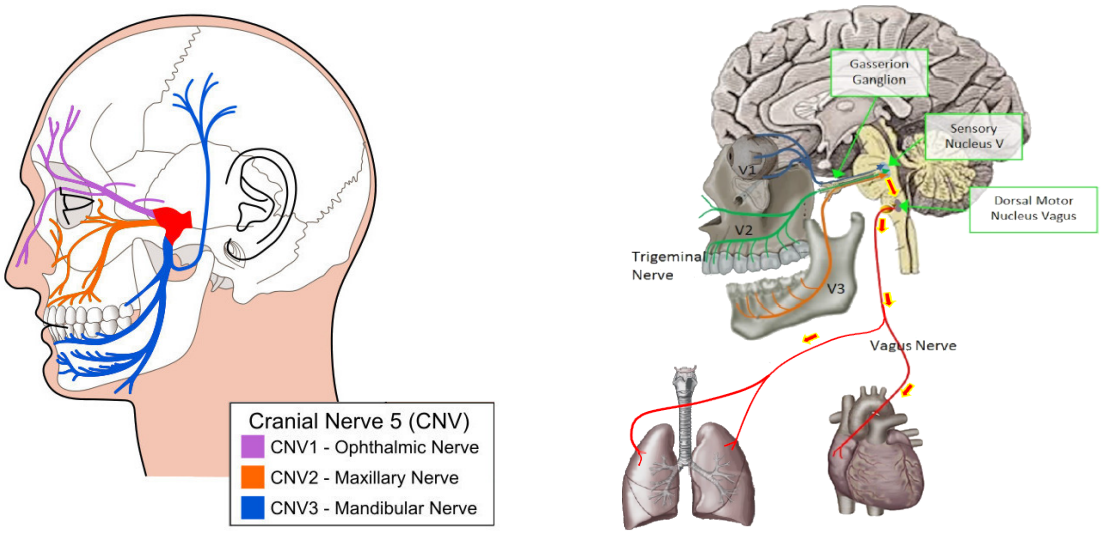

(a) The trigeminal nerve **(b)** Trigeminal and vagal pathways to the brainstem

Figure 2.2: Illustration of the cranial nerves and the trigeminal nerve i.e. the fifth cranial nerve [Inf].

in an oxygen-deficient situation [Lem15]. The procedure of triggering the *DR* by immersing the face in water is illustrated in Figure 2.3a.

The *DR*-induced effects are significantly impacted by the water temperature. In fact, there is an inversely proportional relationship between water temperature and *DR*-induced bradycardia [Sch96]. Additionally, emotional parameters, such as fear, alter the *DR* [Goo94].

The diving response is also referred to as the *diving reflex*. Since the *DR*-induced phenomenon results from several interacting reflexes that occur simultaneously rather than of one reflex, the term diving response was established in literature [And00]. Nevertheless, in this thesis, both names are used interchangeably.

An alternative to triggering the *DR*, that does not include apnoea or active collaboration, is represented by the *Cold Face Test*. Therefore, patients that cannot hold their breath for a longer period of time are also able to trigger the *DR*. Hence, the cold face-induced *DR* can be used as a more standardized procedure compared to the *DR* triggered by facial immersion in water [Nel80].

The *CFT* is executed by applying a cold stimulus to the patient's face (Figure 2.3b). Thus, the cold receptors in the face are stimulated and the trigeminal nerve is consequently excited.

(a) Triggering by the facial immersion in water. **(b)** Execution of the Cold Face Test.

Figure 2.3: Two ways to trigger the *DR*. For measuring the physiological response to the cold face test the electrocardiogram (ECG) was recorded using a wearable ECG sensor fixed with a chest strap.

The assessment of the diving response (e.g. by performing the *CFT*) is a reliable indicator for the correct functioning of the trigeminal-brainstem-vagal reflex pathways. Therefore, it can be used for the diagnosis of a vast variety of diseases that cause neurological disorders (especially disorders of the autonomic nervous system), such as multiple sclerosis [Nel80], familiar dysautonomia [Hil17], diabetes mellitus [Ben76] or Shy-Drager syndrome [Nel80]. In patients with such diseases, the induced bradycardia occurs in a weakly manner or not at all and can therefore be an indicator for a disorder of the *ANS* or a defect in the trigeminal-brainstem-vagal reflex pathways [Nel80].

Chapter 3

Related Work

3.1 Acute Stress Induction

Typically, stress can be divided into acute and chronic stress. Whilst chronic stress consists of repeated occurrences or chronic existence of stressors over a longitudinal period, acute stress is considered to be created by stressors that occur with a lower frequency [Mil94].
In order to observe the reaction of the human body to acute stress it is necessary to induce it in a controlled environment and by a standardized stressor. For that reason, several research groups have proposed different protocols for acute stress induction.
The *Trier Social Stress Test (TSST)* counts to one of the most conducted protocols. Kirschbaum et al. introduced the procedure that consists of a free speech and mental arithmetic in front of an audience. The authors showed that the protocol reliably induces acute stress resulting in a two to four-fold cortisol level, among others [Kir89].
In 2005, Dedovic et al. proposed the *Montreal Imaging Stress Task (*MIST*)* that evokes moderate psychosocial stress by evaluating the performance of a subject in an arithmetic challenge. Based on the *Trier Mental Challenge Test (TMCT)*, a study protocol was developed that includes computerized arithmetic challenges with induced failure. The authors adapted the *MIST* setup so that the whole study could be conducted inside an imaging unit especially for functional magnetic resonance imaging (fMRI) scans. Additionally, they verified that the *MIST* is a reliable tool to investigate the effects of stress perception and processing [Ded05].
Acute stress tests were heavily employed in previous work to investigate the relationships between stress and physical and mental health. For instance, Dagher et al. analyzed the connection between stress and drug addiction. Therefore, they conducted the *MIST* while habitual smokers were undergoing functional *Magnetic Resonance Imaging (MRI)*. They found significantly decreased

neural activity during stress and increased neural activity to drug cues in the smoker group after the stressor occurred. Finally, this work was concluded by the hypothesis that stress increases the perception of drug cues [Dag09].
Lederbogen et al. showed that city living impacts the processing of social evaluative stress in humans. The authors applied the *MIST* to investigate the relationship between urban life and social stress. Finally, they state that urban upbringing poses an established risk factor for psychological disorders [Led11].
Additionally, Mizrahi et al., Soliman et al. and Pruessner et al. applied the *MIST* investigating the role of the limbic system during acute psychosocial stress [Miz12] [Sol11] [Pru08]. All three found strong *MIST*-induced increases in self-reported stress.
In contrast to the previously mentioned work, Geva et al. used the *MIST* to induce psychosocial stress but they did not use any imaging units. The authors investigated the correlation between psychosocial stress and pain reduction and found a connection between stress and pain summation [Gev14].

3.2 Stress Reduction and Biofeedback

As illustrated in Chapter 1, there is a high need for stress intervention methods. Therefore, various methods were recently researched. Below, an exemplary selection of such approaches and reviews is introduced.
Rainforth et al. reviewed over 100 studies that investigated the relationship between stress reduction and blood pressure. They conducted a meta-analysis to compare various stress intervention approaches. Biofeedback, progressive muscle relaxation, stress management training and the Transcendental Meditation Program, a form of yoga, resulted in a decreased blood pressure. Thus, the authors concluded that these methods decrease the stress perception [Rai07].
Accordingly, Chiesa et al. state that *Mindfulness-based stress reduction (MBSR)* reduces ruminative thinking and anxiety. However, it is pointed out by the authors that the specific effects of *MBSR* require further research [Chi09].
Similar to meditation, yoga possesses certain meditative aspects [Sat09]. Satyapriya et al. investigated yoga as a stress intervention method in pregnant women. They recruited 122 healthy pregnant women. The intervention group showed a stress *decrease*, whilst the stress level of the control group *increased*. Thus, they concluded that yoga not only decreases perceived stress but also improves the adaptive autonomic response to stress [Sat09].

In addition to yoga, physical activity possesses stress-reducing properties. A simple hands-on application that exploits this fact is given by patent US20020083122A1 (A.1). This approach compromises a computer and sensor. The subject uses a browser-based interface to enter personal information. Afterwards, a series of stress-reducing exercises is displayed via the interface. The individual is instructed to conduct all exercises whilst the sensor records the compliance of the user. The system then adjusts the exercises accordingly. Finally, patent US5007430A (A.2) relies on a cyclic exercise-relaxation approach whilst the heart rate of the subject is displayed. The subject has to adapt the intensity to increase its heart rate followed by an interval where the intensity is decreased.

Besides yoga, Biofeedback applications for stress reduction, such as the applications mentioned before, were investigated by various researchers. Dillon et al. used a game-style smartphone application and skin conductance Biofeedback to reduce stress. Subjects were randomly assigned to a Biofeedback and control group. The intervention group used the smartphone application for 30 minutes before the *TSST* was conducted for both groups. Results indicate a significantly decreased perceived stress level in the intervention group [Dil16].

In general, *HRV* seems to be a popular measure to reduce stress. Van der Zwan et al. compared *HRV* Biofeedback to conventional mindfulness meditation and physical activity. 76 subjects were recruited and randomly assigned to the three groups. Each group was introduced to the respective intervention method and instructed to conduct their exercises on a daily basis for five weeks. The Biofeedback consisted of paced breathing exercises with an *HRV* Biofeedback device. Finally, the authors concluded that all three approaches are equally efficient in reducing stress [vdZ15].

As pointed out by Goessl et al., *HRV* Biofeedback might also be used to treat anxiety and stress symptoms. In their work, the authors conducted a meta-analysis to investigate the *HRV* effects in detail. The results indicate a significant reduction in self-reported stress and anxiety. Yet, the need for further research is pointed out again [Goe17].

Similarly, a study with 40 subjects was conducted by Lemaire et al. The intervention group used a Biofeedback device that combines rhythmic breathing and self-generated positive emotions along with *HRV* Biofeedback. The authors found significant decreases in stress levels [Lem11].

Weiner and Zimmerman examined the impact of a stress reduction program on blood pressure and the emotional health of hypertensive employees. In addition to conventional stress coping techniques, such as positive emotion refocusing or emotional restructuring, *HRV* Biofeedback was used to enhance the learning and practicing of the previously mentioned techniques. In accordance with Rainforth et al. [Rai07], they found a decrease in blood pressure and improved emotional health [Wei03].

Similarly, Zucker et al. applied *RSA* Biofeedback in patients with post-traumatic stress disorder (PTSD) and found significant PTSD symptom decreases associated with increased *HRV* [Zuc09]. Furthermore, *HRV* Biofeedback was used to improve the performance in patients' competitive anxiety by Lagos et al. or during cognitive stress by Nattiv et al. Both conclude that *HRV* Biofeedback yields in better performances [Lag08] [Pri11].

3.3 Cold Face Test

The *CFT* is a wide-spread application, especially as a supportive measure in the diagnosis and research of neural diseases since it induces vagal excitation [Hil17]. *Familial dysautonomia (FD)*, which is caused by parasympathetic dysfunction, counts to these diseases. Hilz et al. used the *CFT* to investigate the parasympathetic dysfunction in this disorder. They applied a cooling pack for 60 seconds to the forehead and cheeks of *FD* patients. The authors found that the *CFT* induced only slight bradycardia or none in patients with *FD*. Consequently, they concluded that *FD* patients have a reduced parasympathetic response and therefore efferent parasympathetic malfunctioning [Hil17].
A similar approach was applied by Wecht et al. Here, the *CFT* was conducted with people suffering from spinal cord injury. The authors aimed to assess the effect of the lacking physical activity on these subjects. Once again, the authors applied a cooling pack to the face of the subject for 60 seconds. In contrast to a control group, the *CFT*-induced bradycardia differed significantly between young and old subjects with spinal cord injury. Moreover, these subjects showed paradoxical cardiac *CFT*-induced reactions and a lack of vagal activation. Finally, the authors concluded that the abnormal autonomic reactions in subjects with spinal cord injury result not only from the injury itself but also from inactivity [Wec09].
However, the *CFT* aids not only in the diagnosis of diseases that are related to the *ANS*, but can be used to address psychosocial scenarios. Iorfino et al. conducted the *CFT* to investigate its effect in the performance in a social cognition task. The authors hypothesized that the *CFT*-induced vagal excitation yields in increased prefrontal inhibitory control and thus in a better performance during the 'Reading the Mind in the Eyes Test'. However, the results contradicted the theory: Even though the *CFT* induced increased *HRV*, there was no improved performance in the social cognition task [Ior15].
Moreover, the *CFT* was applied in the field of stress research. La Marca et al. conducted the *MIST* to investigate the relationship between the vagus nerve and the *HPA* axis. The authors applied the

CFT to induce vagal stimulation, whilst the *MIST* was conducted to stimulate the *HPA* axis. Hence, the effect of the *MIST* on the *PSNS* was also investigated. Additionally, baseline and *CFT*-induced stimulation scenarios were conducted to assess vagal functioning. The authors concluded that a fast response to the *CFT* goes in hand with a reduced cortisol increase and enhanced mood after acute stress [Mar11].

Chapter 4

Methods

To validate the goal of this thesis, namely analyzing the applicability of the *CFT* as a measure to damp the acute stress response, the physiological response of the human body, both to acute stress and the *CFT* stimulus needs to be captured. Therefore, *Electrocardiogram (ECG)* recordings and saliva samples were collected throughout the whole process. In this chapter, the applied methods, including the *CFT* procedure and the feature derived from the acquired data, are described in detail.

4.1 Cold Face Test

In this thesis, the *CFT* was carried out by applying a cooling mask (Dr. Winkler GmbH, Ainring-Mitterfelden, Germany). The duration and number of subsequent cold face exposures were evaluated in a pre-study (see Section 5.2). As shown in Figure 2.3b, the mask covers most facial areas with openings for the eyes, nose and mouth. Therefore, normal breathing was ensured whilst triggering the occulocardiac reflex by applying pressure on the eyes was avoided [Mar11]. The cooling mask was applied with a temperature of -1°C. An additional cooling mask (-14°C) was applied to the first one to prevent it from warming up too quickly. During the procedure, the subject sat upright on a chair and was instructed not to move or talk while continuing spontaneous breathing. Before the cold exposure, a 60 second baseline interval was recorded to assess the impact of the *CFT* in comparison to the resting values.

4.2 Data Acquisition

To measure the activity of the *HPA* axis, saliva samples were collected and cortisol levels were determined. Additionally, a wearable sensor (Portabiles GmbH, Erlangen, Germany) containing an inertial measurement unit (IMU) and an *ECG* sensor, was used. It was attached to the chest of the subject and recorded data throughout the whole study procedure. *ECG* was recorded according to Lead II of Einthoven's triangle [Lan07]. The negative electrode was placed on the sternum whilst the positive one was placed on the left hand side of the costal arch (Figure 4.1).
In addition to the *ECG* signal, acceleration and gyroscope were recorded. Since a chest strap was used to fix the sensor node to the thorax (see Figure 2.3b), the cyclic movements of the rib cage were recorded. Therefore, respiratory cycles could be extracted from the recorded accelerometer data.
All sensor data was logged onto the internal storage of the sensor with a sampling frequency of 256 Hz. After data collection, the recorded sessions were transmitted as binary files to a smartphone application[1] via Bluetooth Low Energy (Figure 4.2). On a PC the binary files were then imported for data analysis into Python using the Python library *NilsPodLib*[2].

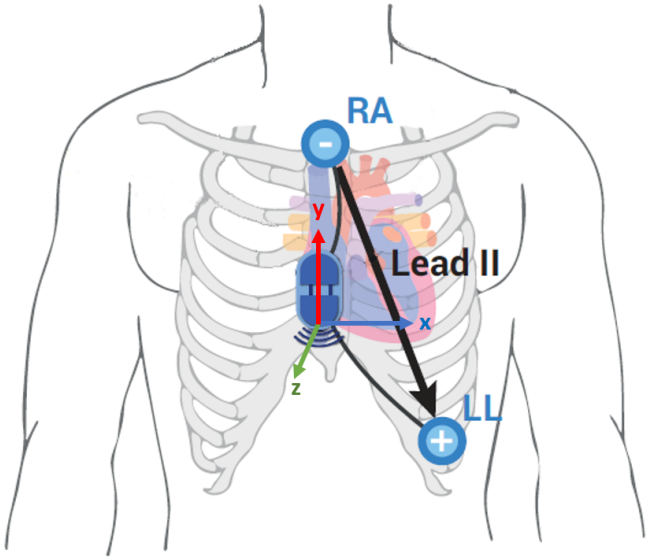

Figure 4.1: Lead II according two Einthoven's triangle. Modified from [Ric15]

[1] PortabilesDemoApp, Portabiles GmbH, Erlangen, Germany, https://play.google.com/store/apps/details?id=de.portabiles.demoapp
[2] NilsPodLib https://mad-srv.informatik.uni-erlangen.de/MadLab/portabilestools/nilspodpythonlib

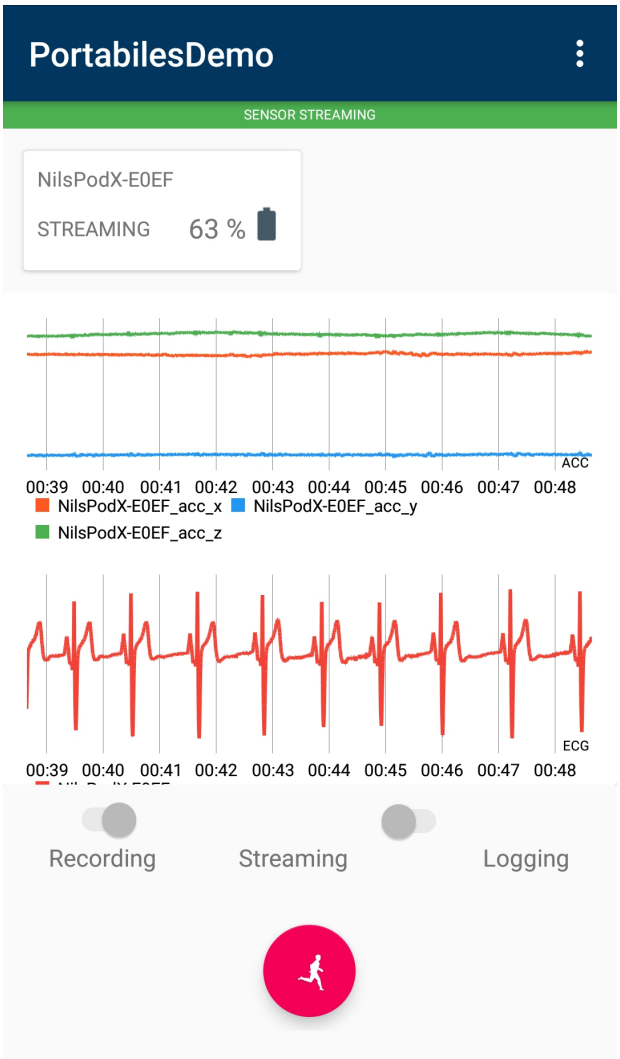

Figure 4.2: Android application for controlling the sensor. Accelerometer data (upper section) and *ECG* data (lower section) can be streamed in real-time (as depicted in the screenshot) or logged onto the internal sensor storage.

4.3 Data Processing

The primary goal of this thesis was the assessment of the *CFT* as a stress reducing measure. Thus, various *HRV* features were computed and analyzed. In general, *HRV* features split into three groups: time-domain, frequency-domain and non-linear features. Below, these different groups are introduced based on the work of Sammito et al. and Malik et al. [Sam14] [Mal96].
Time-domain strategies usually deploy statistical or geometric procedures. While the later use geometric forms, such as bar graphs, for analysis, statistical methods evaluate inter-beat intervals with regard to their variance. Frequency-domain *HRV* measures, such as Fast-Fourier Trans-

formation, auto-regression, zero-crossing-methods or wavelet analysis, fall back on frequency analysis. Thus, these approaches exploit the fact that different physiological processes dominate in different frequencies and amplitudes. In contrast to time- and frequency-domain characteristics, non-linear features, such as detrending methods or the Poincaré Plot, typically do not assess *HRV* quantitatively but rather qualitatively [Sgo15].
Due to the fast cardiac recovery after the end of the cold stimulus to the face, only a rather short *ECG* interval is of interest to assess the *CFT* effect. Thus, only time-domain and non-linear features were concerned. In Table 4.1, used *HRV* features along with a short definition are displayed, whereas a closer description paired with computational information is given in the section below. Python's NumPy module[3] was used frequently in the implementation of the subsequent *HRV* features.

Table 4.1: Selection of *HRV* features [Mal96].

Abbreviation	Definition	Unit	Indicator for
	time-domain parameters		
RMSSD	Square root of the mean of all squared differences of successive RR-Intervals (see Equation 4.1)	ms	*PSNS*
RSA	Difference of the maximum RR-Interval during expiration and minimum RR-Interval during inspiration	ms	*PSNS*
RR50	Number of successive RR-Intervals that differ by more than 50 ms	N/A	*PSNS*
pNN50	Percentage of successive RR-Intervals that differ by more than 50 ms	%	*PSNS*
	non-linear parameters		
SD1	Standard deviation of the distances to the longitudinal diameter	ms	*PSNS*
SD2	Standard deviation of the distances to the transverse diameter	ms	*SNS*, *PSNS*

4.3.1 R-Peak Detection

First, the recorded ECG signal was filtered using a second-order FIR-bandpass filter (3 - 45 Hz) to reduce noise, such as powerline interference or baseline drifts. Second, the R-Peak detection algorithm according to Hamilton et al. [Ham02] was applied to the filtered *ECG* signal using

[3] numPy 1.16.3, `https://numpy.org/`

the *ECG* module of *BioSSPy* [4]. An exemplary section of the signal with detected R-Peaks is shown in Figure 4.3. Subsequently, the differences between two successive R-Peaks, i.e. the RR-Intervals, were computed. As a next step, artifacts in RR-Intervals were reduced using the *NeuroKit* library[5]. Therefore, all RR-Intervals were z-normalized and replaced by the value of a ten-point moving average of the preceding RR-Intervals if they were above or below a threshold of 1.96 (corresponding to the 2.5% upper and lower RR-Intervals, respectively).

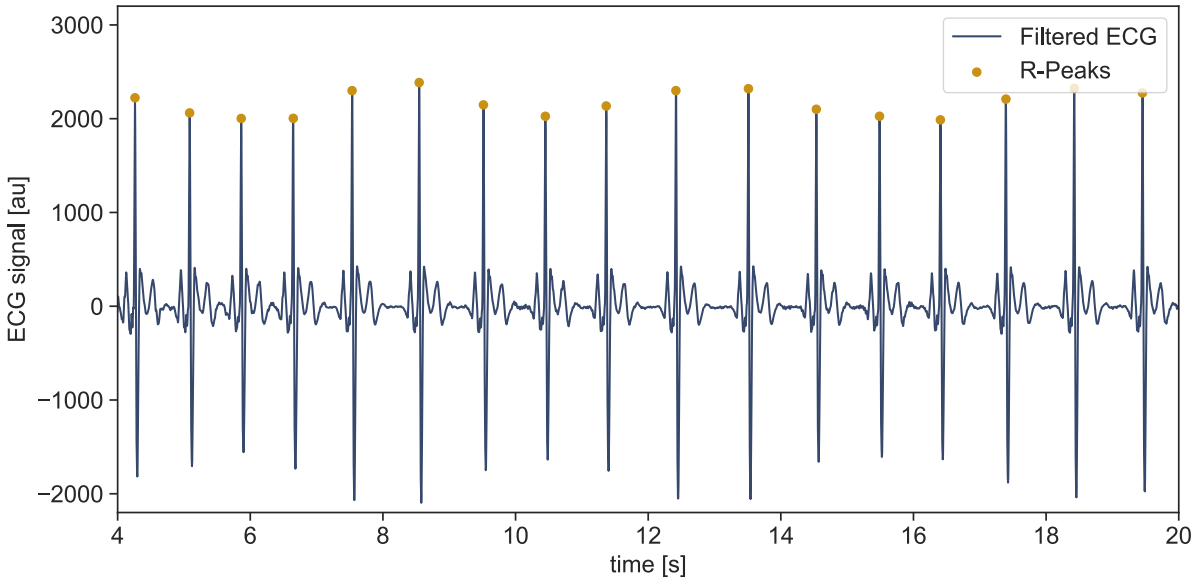

Figure 4.3: R-Peak detection performed on a section of an *ECG* signal.

4.3.2 CFT-specific features

The CFT *onset* is defined as the first occurrence of three successively slowing heartbeats, i.e. heart beats that are below the pre-*CFT* assessed heart rate baseline [Khu06], whereas the point of *peak bradycardia* indicates the minimum *HR* between *CFT* onset and the end of cold exposure. Thus, the onset was the result of three successive RR-Intervals that were on average above baseline. An exemplary illustration of the detected points along with the *CFT*-induced increasing RR-Intervals is shown in Figure 4.4.

[4] BioSPPy 0.6.1, `https://biosppy.readthedocs.io/en/stable/`
[5] NeuroKit 0.2.0, `https://neurokit.readthedocs.io/en/latest/`

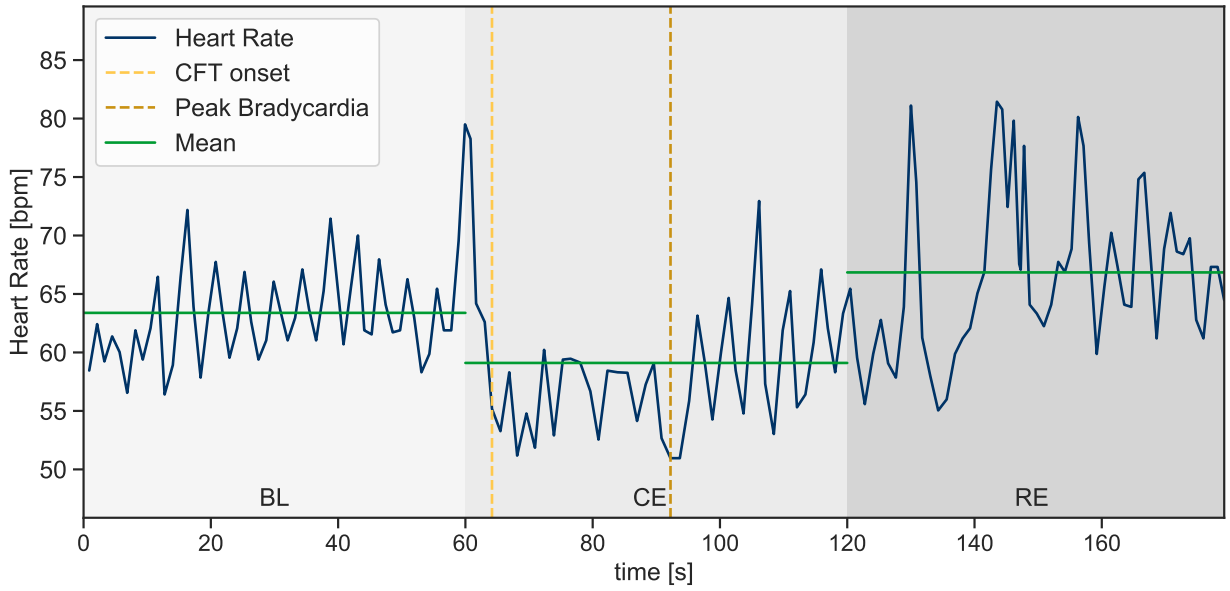

Figure 4.4: HR during the conduction of the *CFT*. After conduction of the baseline interval (BL), the HR decreases during cold exposure (CE) and normalizes during recovery (RE).

4.3.3 RMSSD

The *Root Mean Square Of Successive Differences (RMSSD)* is computed over a window according to Equation 4.1, where RR_i represents the RR-Interval at time point i and N represents the number of RR-Intervals in the window. For this work, a sliding window with N=10 samples was used. Therefore, each point of the *RMSSD* signal displays the value of the preceding ten RR-Intervals (Figure 4.5).

$$RMSSD = \sqrt{\frac{1}{N-1}\sum_{i=1}^{N-1}(RR_{i+1} - RR_i)^2} \tag{4.1}$$

4.3.4 RR50 / pNN50

The *Number Of Successive RR-Intervals differing more than 50 ms (RR50)* results from the computation of differences between successive RR-Intervals in a certain window. Similar to the *RMSSD*, a moving window with a window size of N=10 is applied. Thus, the *number* of differences larger than a threshold of 50 ms is determined for each window. The *Percentage Of*

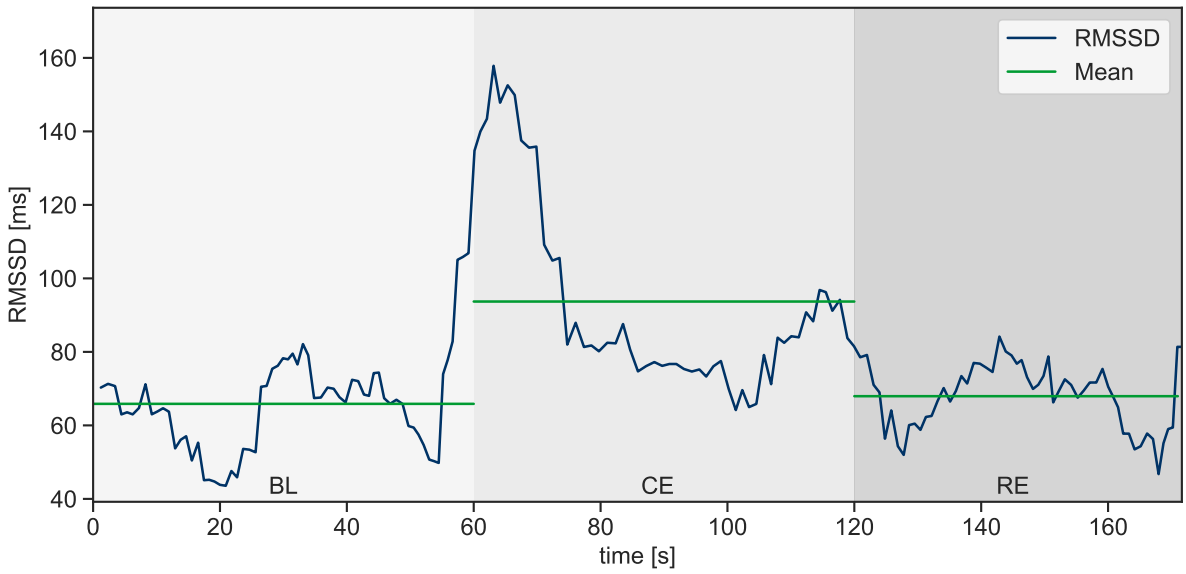

Figure 4.5: *RMSSD* during the *CFT*. The strong increase during cold exposure (CE) indicates higher parasympathetic activation than during baseline (BL) and recovery (RE).

Successive RR-Intervals differing more than 50 ms (pNN50) (Figure 4.6) is computed likewise. However, the *percentage* of RR-Interval differences above 50 ms is computed for non-overlapping windows of ten RR-Intervals.

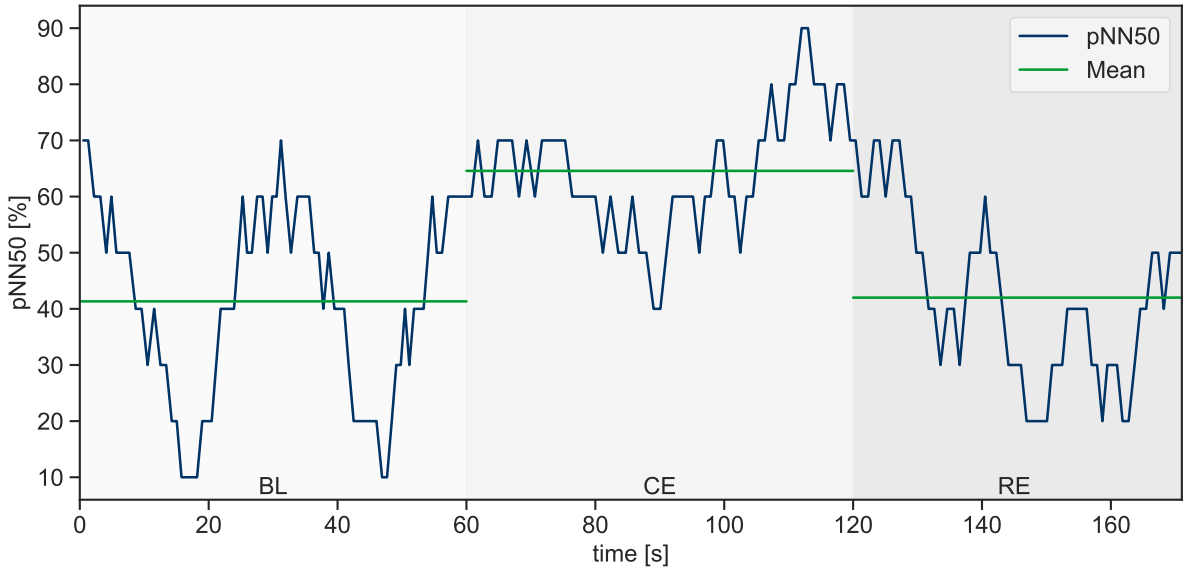

Figure 4.6: *pNN50* during the *CFT*. The clear increase during the application of the cooling mask (CE) indicates higher activation of the *PSNS* than during baseline (BL) and recovery (RE).

4.3.5 Respiratory Sinus Arrhythmia

RSA depicts the *HR* fluctuations accompanying its respiration phases, i.e. inspiration and expiration. There are various methods to determine *RSA* including frequency-analysis or detrending methods. In this thesis, the *peak-valley* method was used [Gro90].
As the sensor node was attached to the subject's chest (Figure 2.3b), lateral thorax movement due to inspiration and expiration is visible as a sinusoidal wave in the z-axis of the acceleration signal (see Figure 4.2). Therefore, this axis can be used to extract a respiration signal for computing the *RSA*.
An adapted version of the respiration function provided by the *BioSPPy* Python module[6] was used to realize the extraction of respiration phases. This method poses a gradient-based approach. First, the raw signal was filtered with a second-order Butterworth bandpass filter ($0.1 - 0.35$ Hz). Second, the gradient of the raw respiration signal was calculated. Third, zeros in the gradient, illustrating local extremes in the respiration signal, were determined. Fourth, inspiration and expiration periods were identified based on the sign of the gradient. Afterwards, the start of the respective respiration phase was detected as local minima posed starting inspiration phases and local maxima beginning expiration phases. Finally, inspiration phases that were shorter than 1 s and expiration phases that are shorter than 1.25 s were rejected. Both thresholds result from 50% of typical resting inspiration ($1 - 2$s) and expiration phases ($2.5 - 3.5$s) [Sch13]. Figure 4.7a shows the result of the algorithm and the detected respiration phases.
For computing the actual *RSA* values, the *peak-to-valley* method of the NeuroKit Python module[7] was used. Firstly, RR-Intervals were computed for inspiration and expiration phases, respectively. Finally, the difference between the maximum RR-Interval during expiration and the respective minimum interval were computed. If no RR-Interval was determined in a certain phase, the *RSA* value at the respective point was set to 0. Afterwards, the resulting signal was interpolated with a third order spline function resulting in a continuous *RSA* signal as shown in Figure 4.7b.

4.3.6 SD1 and SD2

The Poincaré Plot displays each RR-Interval as a function of the successive RR-Interval. In contrast to time- or frequency-based *HRV* analysis methods, the Poincaré Plot does not require stationary or quasi-stationary input signals since it rests upon the notion of different temporal changes in the *HR* [Mou04].

[6] BioSPPy 0.6.1, `https://biosppy.readthedocs.io/en/stable/`
[7] NeuroKit 0.2.0, `https://neurokit.readthedocs.io/en/latest/`

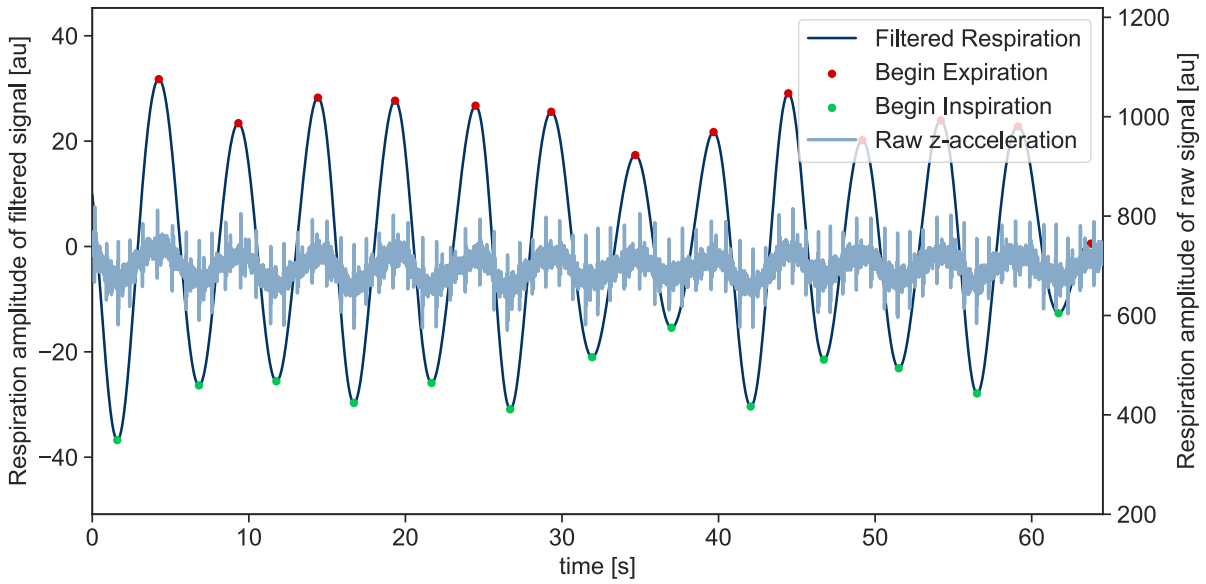

(a) Section of the final signal with the detected respiration intervals.

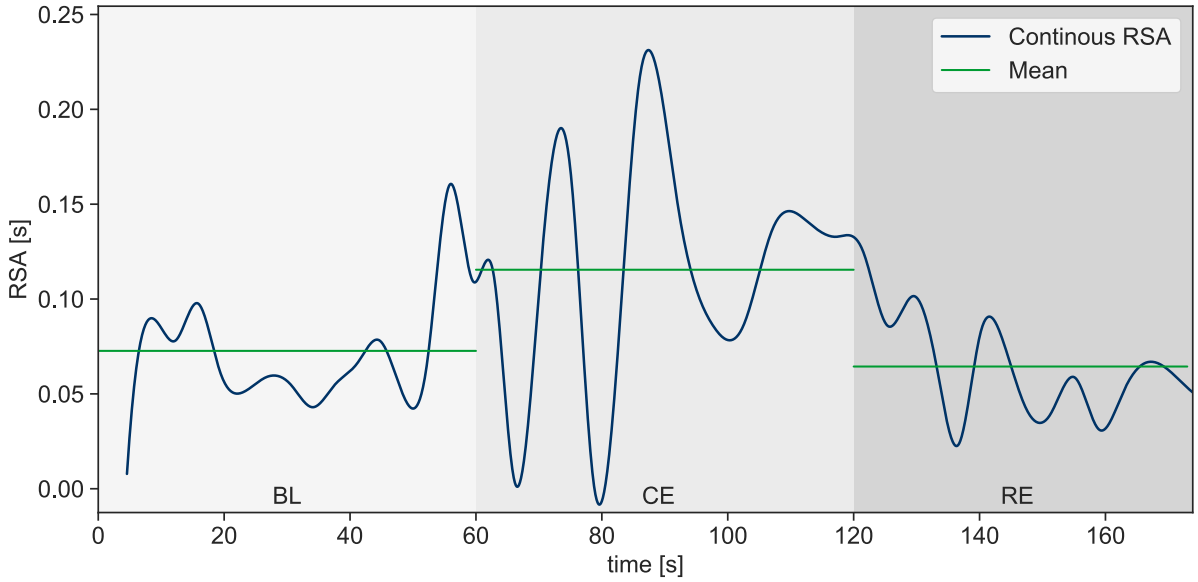

(b) *RSA* during the *CFT*.

Figure 4.7: Respiration Extraction and *RSA* determination. The decreases in *RSA* around 65 s and 80 s result form the absence of a minimum or maximum RR-Interval during the respective respiration phase.

In the analysis, an ellipse is fitted to the point cloud according to following algorithm [Tul96]: Firstly, the center of the ellipse is placed such that it coincides with the center of the point cloud. Then, the orientation of the ellipse is determined based on the slopes of the principal axes in

transverse and longitudinal direction. Last, the height of the ellipse is defined by the standard deviation of the *longitudinal* axes after rotating the plot 45° clockwise (SD1). In parallel, the width of the ellipse is determined by the standard deviation of the *transverse* axes after rotating the plot 45° counter-clockwise (SD2) [Tul96].
An exemplary plot is illustrated in Figure 4.8. A more detailed description of the fitting process and a closer illustration of the computation of the standard deviations, including mathematical background and formulas, is given by Brennan et al. [Bre01].
The SD1 feature indicates only parasympathetic modulations [Mal96]. On the contrary, the SD2 feature is assumed to include both sympathetic and parasympathetic aspects. Thus, SD2 does not allow a direct interpretation of one of the two *ANS* pathways. The ratio of SD1 and SD2 is computed additionally, thus enabling to better assess parasympathetic activity as the parameter *SD1*, i.e. the activity of the *PSNS*, is set into context to the total activity of the *ANS* [Sam14]. Several other features can be extracted from the Poincaré Plot, however, they do not pose clear attributes of either the *PSNS* or *SNS* [Sam14].

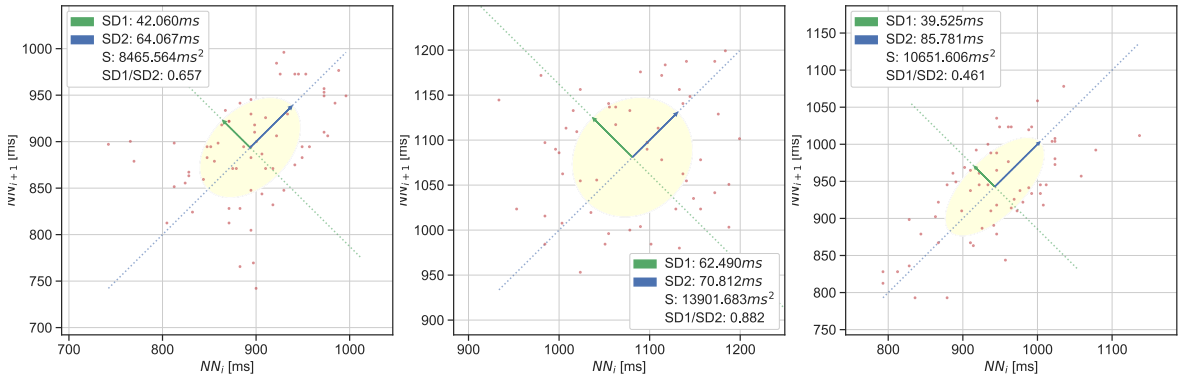

(a) Baseline **(b)** Cold Exposure **(c)** Recovery

Figure 4.8: Poincaré Plot of RR-Intervals. The red points display the RR-Intervals. The area of the ellipse (S), both standard deviations and their ratio are displayed in the legend.

4.3.7 Cortisol-derived features

Derived from the "raw" cortisol concentrations the *Area under the curve with respect to ground (AUC-G)* (Figure 4.9a) and *Area under the curve with respect to increase (AUC-I)* (Figure 4.9b) were computed. The *AUC-G* displays the total amount of secreted cortisol, whilst the *AUC-I* takes the difference between the single measurements into account [Pru03]. The *AUC-G* is

computed according to Equation 4.2. The formula for computing the *AUC-I* is identical to the *AUC-G*-formula except for the removal of the area between ground and the first sample (S1) for all points (Equation 4.3) [Pru03]. In addition to the areas under the curve, the difference between the pre-*MIST* (S1) cortisol concentration and the peak level (S4) was computed. Moreover, the slope between both points was also determined by Equation 4.4 (Figure 4.9c).

$$AUC_G = \sum_{i=1}^{n-1} \frac{(m_i + m_{i+1}) \cdot t_i}{2} \tag{4.2}$$

$$AUC_I = AUC_G - m_1 \cdot \sum_{i=1}^{n-1} t_i = \sum_{i=1}^{n-1} (\frac{(m_{i+1} + m_i)}{2} - m_1) \cdot t_i \tag{4.3}$$

$$S1\text{-}S4\text{-}Slope = \frac{m_4 - m_1}{t_4 - t_1} \tag{4.4}$$

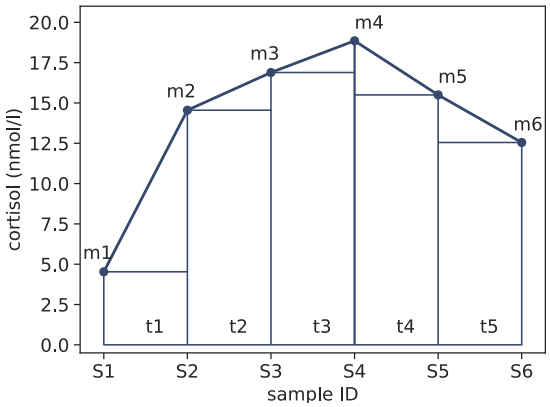

(a) *AUC-G*

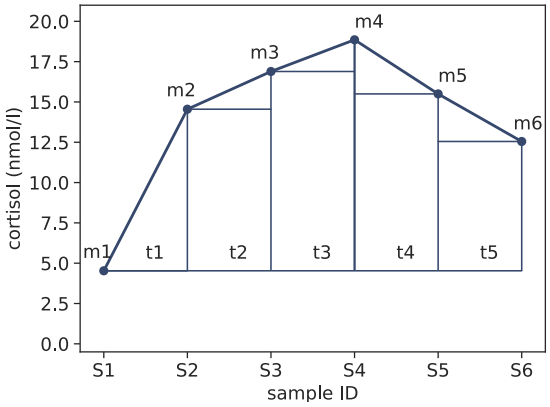

(b) *AUC-I*

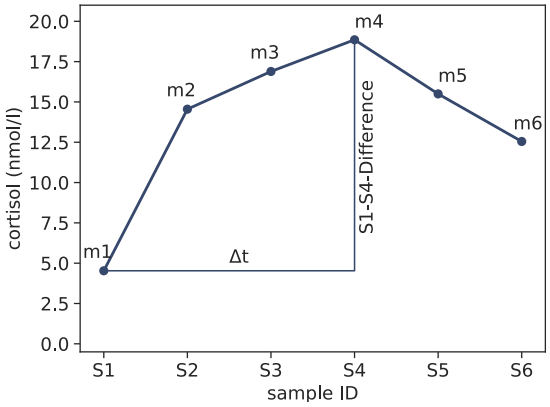

(c) S1-S4-Difference

Figure 4.9: Cortisol-derived features. The *AUC-G* displays the total amount of secreted cortisol, whilst the *AUC-I*, S1-S4-Difference and the according slope rather display the *MIST*-induced cortisol increase.

Chapter 5

Evaluation

In this chapter, the MIST is introduced as a measure to evaluate the effect of the CFT on the stress system and a detailed description of the conducted study is given. Last, recorded measures and statistical analyses used for the evaluation of the results are illustrated.

5.1 Montreal Imaging Stress Task

The introduction of the *MIST* protocol is based on the work of Dedovic et al [Ded05]. The *MIST* was actually developed as a measure to evaluate the impact of moderate stress on brain activation. For this reason, the *Trier Mental Challenge Test* (*TMCT*) was modified so that the whole procedure can be conducted inside an imaging unit, for instance, a *MRI* or *Positron Emission Tomography (PET)* unit.
The *MIST* protocol typically consists of mental arithmetic challenges paired with a social evaluative threat. The former component is typically built into a computer program that presents the principal component of the *MIST* whereas an investigator scrutinizing the performance of the subject poses the social stressor.
The program displays arithmetic tasks. Subjects are instructed to solve them by using a rotary dial to enter the solutions. Immediate feedback to each answer ('Correct' or 'Incorrect') is displayed in an interaction field. The tasks are created by using up to four double-digit numbers and up to four operators (addition, subtraction, multiplication and division). Regardless of the difficulty, the answer will be a single-digit number.
In general, three conditions (*Rest, Control and Experimental*) are conducted. During the *Rest* condition, the computer program interface is shown. However, no tasks are displayed. This phase is used to accustom subjects to the study environment. During the *Experimental* condition, various

evaluative components, for instance, a performance evaluation bar and a timeline, are displayed. The evaluation widgets refresh with each given answer with a neutral or threatening sound signal occurring depending on whether the given answer is correct or false. The performance bar indicates the feat of the user. Additionally, an indicator shows a fictional average performance of other participants that ranges constantly between 80%−90%. Furthermore, subjects only have limited time to enter their solution. Otherwise, the negative sound also occurs and appropriate feedback ('timeout') is displayed via the interaction field. In contrast to the *Experimental* condition, there are no evaluative tools shown in the *Control* condition. Here, subjects get used to the *MIST* interface and the rotary dial. In Figure 5.1 the interface during the *Experimental* condition is illustrated.

Each condition is divided into three sections, each with a duration of four minutes. After each interval, a study instructor informs the subject about its performance. During the first feedback interval, the subject is reminded that a minimum feat is required and that his or her performance

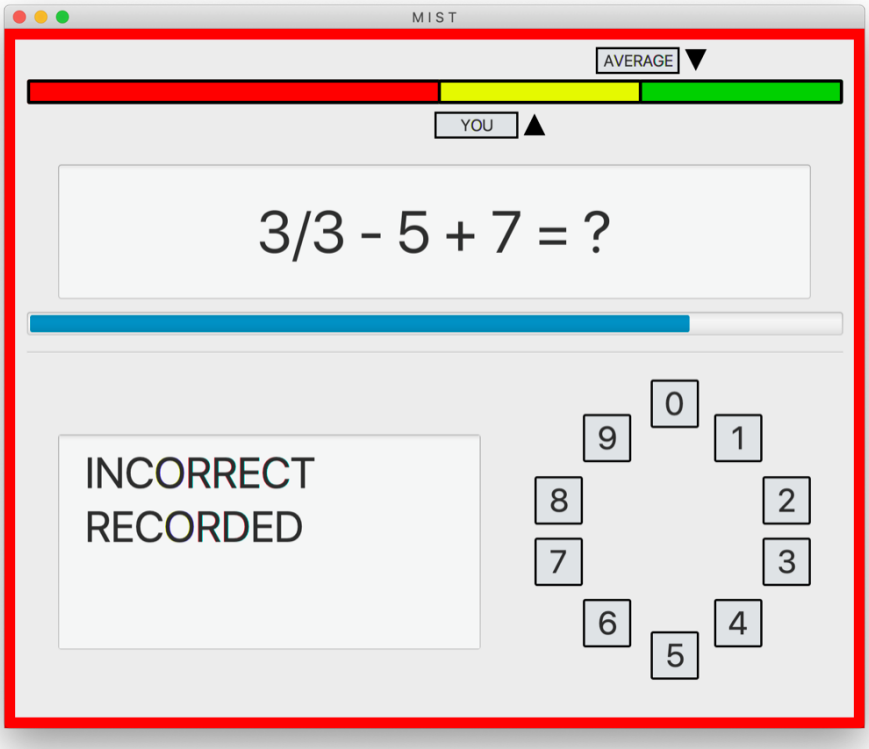

Figure 5.1: Computer Interface of the *MIST*. The top bar indicates the individual and average performance, below the arithmetic task and timeline is shown. In the bottom half, the interaction field and the rotary number pad are displayed. Based on [Ded05].

must be close to the average to be used in the study. Last, the rotary dial is explained again and the subject is instructed to repeat the test. In the second feedback interval, the instructor enters the room and informs the subject about its repeated poor performance. Additionally, a fictional study leader enters the room and interrogates the participant about personal problems (e.g. school performance). Afterwards, the subject is informed about the high costs and expenses of the study. Finally, the study leader and instructor stay in the room and ask the subject to repeat the test once again. After finishing the third block, subjects are debriefed.

5.2 Study Design

In contrast to the original *MIST* version that was introduced above, the *Control* condition was used only for a two minute tryout interval prior to the *Experimental* condition to accustom the subject to the interface. Additionally, the time limit for each arithmetic task was set in accordance to the difficulty of the respective task (level 1 - level 7). Moreover, the average difficulty of the challenge was set prior to each interval. A high difficulty was chosen ensuring a high failure rate. Each interval began with a task of mediocre difficulty. If the subject answered the previous tasks correctly, the difficulty of the next task increased. Contrarily, the difficulty decreased only if three successive answers were answered incorrectly. Thus, the performance of the participant is typically outperformed by the fake average performance. Finally, subjects used a computer mouse to select their solution on the rotary number pad.
To maintain the impartiality of the subjects, they are told that the study investigates the correlation of cognitive performance and stress mediated by environmental influences, such as the audio signal or the cooling mask.
Prior to the actual study, a pre-study was conducted that aimed to determine the optimal *CFT* parameters. The investigated parameters included different exposure times and a different number of repeated exposures. Five participants were involved in the pre-study (one female, four males). As the *MIST* consists of three intervals, there are up to three possibilities, i.e. prior to each run, that allow interaction with the subject. Thus, up to three repeated cold applications were investigated. As shown in Table 5.1, the *CFT* effect appears to be more prominent in the 60 s exposure group. However, the comparison of both procedures showed that the *CFT* induced bradycardia lasted longer during the 120 s cold exposure (Figure 5.2). Even though the average stimulation in the 120 s exposure group seems to be weakened, a longer lasting bradycardia may indicate longer parasympathetic stimulation. As no clear differences between the single repetitions showed, the exposure duration was set to 120 s and the number of repetitions was set to three.

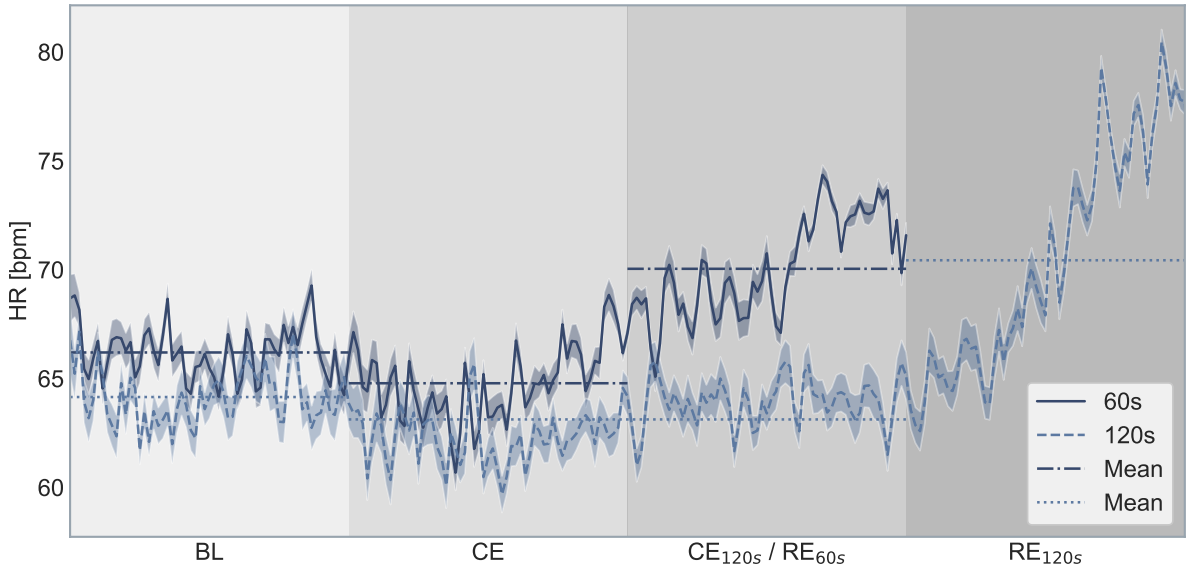

Figure 5.2: *HR* course during the pre-study. Both groups were exposed to the same protocol: 60 s baseline (BL), 60 s or 120 s cold exposure (CE) and 60 s recovery (RE). The induced bradycardia is clearly maintained in the two minute group during the second half of exposure.

Table 5.1: *HRV* results based upon data acquired during the pre-study.

	Mean *HR* Decrease	**Max *HR* Decrease**	***HR* above Baseline**
1^{st} 60s exposure	$11\% \pm 7\%$	$25\% \pm 9\%$	$16\% \pm 17\%$
2^{nd} 60s exposure	$6\% \pm 6\%$	$20\% \pm 9\%$	$30\% \pm 17\%$
3^{rd} 60s exposure	$2\% \pm 6\%$	$19\% \pm 10\%$	$42\% \pm 20\%$
1^{st} 120s exposure	$2\% \pm 4\%$	$19\% \pm 5\%$	$39\% \pm 19\%$
2^{nd} 120s exposure	$4\% \pm 3\%$	$19\% \pm 3\%$	$29\% \pm 14\%$
3^{rd} 120s exposure	$0\% \pm 2\%$	$16\% \pm 6\%$	$56\% \pm 14\%$

Subjects were recruited in lectures at the University of Erlangen-Nuremberg. Exclusion criteria included psychiatric disorders, the consumption of psychoactive substances, excessive consumption of alcohol (>2 alcohol beverages per day) or tobacco (>5 cigarettes per day). In total, 35 subjects were recruited, but four subjects were excluded from the study since they failed the medical questionnaire that was conducted prior to the study checking for any diseases or medication intake

Table 5.2: Demographic distribution of the study groups

	Age [years]	Height [cm]	Weight [kg]
Control	20.64 ± 2.27	173.14 ± 6.60	66.86 ± 11.11
CFT	19.62 ± 2.63	170.38 ± 7.92	59.05 ± 7.55

that might affect the stress response, such as anti-inflammatory drugs. Additionally, two subjects did not appear. Participants were asked to avoid the consumption of alcohol on the day before the study and the day of the study. Furthermore, they were asked to get up at least three hours prior to the study. Subjects were randomly assigned to either the Control group or the group that was exposed to the *CFT*. In Table 5.2, the mean age, weight and height of each group is displayed. The study took place between 11:00 a.m. - 5:30 p.m. After arriving at the laboratory and completing the informed consent, the first saliva sample was taken (see Figure 5.3). Salivettes (Sarstedt AG & Co. KG, Nümbrecht, Germany) were handed out for this purpose and subjects were instructed to chew on the cotton pad for two minutes. For all subjects the *MIST* took place in the same room at a room temperature of 21 °C. Additionally, all subjects used the same computer. Firstly, subjects were equipped with a sensor node and seated in a chair. After resting for 15 minutes and answering the demographic (D) and medical (M) questionnaires, subjects had to answer a

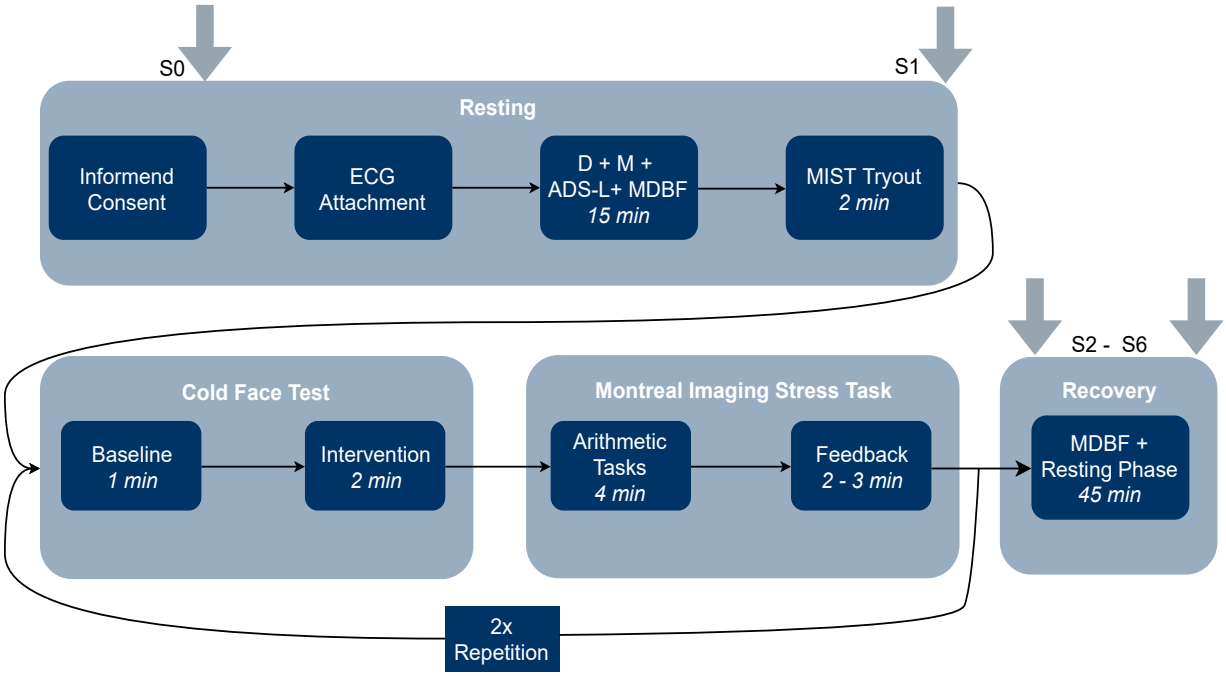

Figure 5.3: Protocol of the evaluation process. *Note:* D: demographic questionnaire, M: medical questionnaires

depression questionnaire (*German version of the Center for Epidemiologic Studies Depression Scale (ADS-L)*) [Hau92] and a mood questionnaire (*German version of the Mulitdimensional Mood State Questionnaire (MDBF)*) [Ste97]. Subsequently, a two minute tryout interval was completed. Afterwards, the *CFT* was carried out with the respective group and the *MIST* Experimental condition was conducted with both groups. After each Feedback interval, the *CFT* was repeated with the *CFT* group. Once the *MIST* was finished, participants were asked to answer the *MDBF* questionnaire again and stayed for an additional 45 minutes. Finally, subjects were debriefed and received either a certificate of participation or 20 €.
In addition to the first saliva sample, further samples were taken as shown in Table 5.3. Subsequently, the samples were kept at room temperature until the end of each session. Afterwards, they were stored in a refrigerator with an approximate temperature of -20°C for later analysis in the laboratory.

Table 5.3: Times relative to the *MIST* start where saliva samples were taken.

Saliva sample	S0	S1	S2	S3	S4	S5	S6
time [min]	-27	-1	30	40	50	60	70

5.3 Measures

Questionnaires

Besides the *MDBF* that was conducted to provide qualitative assessments of stress, demographic and medical questionnaires were assessed primarily for subject exclusion. Former consisted of general questions about age, weight, height and gender, whilst latter included questions about medication intakes and preexisting diseases.

Electrophysiological Measures

The *ECG* was recorded to assess the effect of stress and cold-face stimulation on the cardiovascular system. Derived from the *ECG*, *HRV* features like *RMSSD*, *RSA*, *pNN50*, and SD1/SD2 ratio were computed. Moreover, the time above baseline, and latency until baseline is reached were derived from *HR*, *RSA*, *RMSSD*, and *pNN50* (Table 5.4). These measures were computed for the global (mean of the signal recorded during the resting phase) and local baseline (mean of the one minute interval prior to the intervention phase). The mean of each variable was determined

for all *MIST* phases and all sub-phases, i.e. *Baseline*, *Intervention*, *Arithmetic Tasks* and *Feedback*, and for the *Resting* and *Recovery* phase. The *Feedback* interval and *Recovery* phase were generally not taken into consideration as there was no strict framework and thus variations, for instance in length, occurred. Moreover, *RSA* was disregarded during the analysis due to uncertainties in the respiration extraction.
Moreover, the relative change with regard to the respective global baseline (recorded during the resting phase) was computed for all measures. Then, the median, confidence interval and significance of difference was determined for all subjects and all groups.

Feature	time above global baseline	time above local baseline	latency to global baseline	latency to local baseline
Symbol	$\hat{t}_{glo}$	$\hat{t}_{loc}$	τ_{glo}	τ_{loc}
Unit	%	%	s	s

Table 5.4: Feature-derived measures.

Cortisol

The first saliva sample (S0) was disregarded from further analysis as it was only recorded for subject exclusion and baseline comparisons. Derived from the raw cortisol values, the *AUC-G* and *AUC-I* were calculated [Pru03]. Both measures were computed over all cortisol values (S1-S6) and over all values after the MIST (S2-S6). Additionally, the difference between S1 and S4 and the respective slope were determined.

Statistics

Mixed-measurement *Analysis of Variance (ANOVA)* was used to determine possible interaction effects, whilst univariate *ANOVA* was used to determine significance levels between groups. As post-hoc test the Tukey HSD (Honestly Significant Difference) test was conducted. Prior to the application of *ANOVA*, homogeneity of variances was assessed by the Levene test and Greenhouse-Geiger corrections were applied if the assumption of sphericity (Mauchly Test), was violated. The significance level was set at $p < 0.05$. Effect sizes are reported as η_p^2 with 95% confidence intervals. All methods utilized are provided by the *Pingouin* Python module[1].
Linear regressions between the single *MIST* repetitions were calculated to determine possible trends over time. *ANOVA* was then used to test for significant differences.

[1] pingouin, 0.3.0, https://pingouin-stats.org/index.html

Chapter 6

Results

All results that have been gathered within this thesis are illustrated in this chapter. One subject was excluded from further analysis as it did not respond to the *CFT* (and even showed a heart rate increase) when none or only moderate stress was induced. Additionally, one subject was excluded due to highly elevated initial cortisol levels. The remaining 26 subjects (13 subjects per group) completed all three *MIST* phases.
For analysis, all electrophysiological features were normalized with regard to the resting baseline of the respective subject. Thus, the effect of subject-depended resting heart rate differences was reduced. Consequently, all resulting *HR(V)* features must be interpreted as changes relative to the resting baseline.

6.1 MIST Responses

6.1.1 Electrophysiological Measures

During all *MIST* phases, the *HR* showed increases starting with the begin of the *Arithmetic Tasks (AT)*, reaching its peak after about one third of the *AT* interval (Figure 6.1). Moreover, the *HR* remained at this peak level (or decreased only slightly) for the second and third *MIST* phase. This effect is even prominent throughout the Feedback interval. Furthermore, most of the *HRV* features showed a significant interaction of sub-phase by *MIST* phase. Additionally, significant differences in *HR* occurred between the single *MIST* phases (Table 6.1). *Post hoc* testing showed a significant increase in *HR* between the first and last *MIST* phase ($p < 0.001$), but not between the other phases (*MIST*1-*MIST*2: $p = 0.132$, *MIST*2-*MIST*3: $p = 0.061$). Similarly, *post hoc* testing separately in each *MIST* phase showed significant decreases in *RMSSD*, *pNN50*, and SD1/SD2 (Table 6.2).

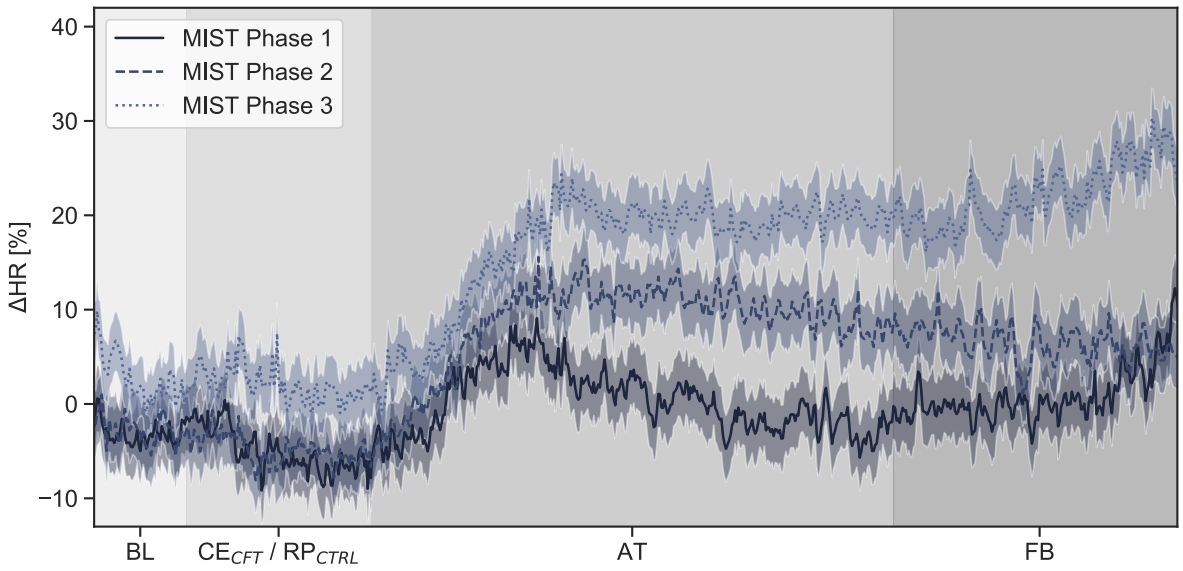

Figure 6.1: Process of the *HR* during the conduction of the *MIST*. Each *MIST* phase consists of a Baseline (BL), Cold Exposure Intervention / Resting Period (CE/RP), Arithmetic Tasks (AT) and Feedback (FB) interval.

The courses of *HR* shown in Figure 6.1 indicates a *HR* increase (peak as well as mean values) throughout the *MIST* phases. Whilst the *HR* maximum in the first phase increased by about 10%, it showed increases of 12% and 25% in Phases 2 and 3, respectively. During the first *MIST* phases, the *HR* returned rapidly to the baseline level at the end of *AT*, with a slight *HR* increase during Feedback (FB). Moreover, the *HR* during the second phase decreased only slightly after reaching the peak level and even remained constant during the last interval. Here, the Feedback interval actually induced an increase in *HR*.

Table 6.1: *ANOVA* results of *HRV* analysis (interaction sub-phase by *MIST* phase). *Note:* between: sub-phase, within: *MIST* phase; df_{Num}: degrees of freedom of the numerator, df_{Den}: degrees of freedom of the denumerator; ^{s}: the main effect of the sub-phase (BL vs. AT); $^{*}p < 0.01$, $^{**}p < 0.01$, $^{***}p < 0.001$.

Dependant Variable	df_{Num}, df_{Den}	F	p	η_p^2
HR ^{s}	1, 50	8.68	0.048^{*}	0.15
RMSSD	2, 100	536.94	$< 0.001^{***}$	0.92
pNN50	2, 100	1098.32	$< 0.001^{***}$	0.96
SD1/SD2	2, 100	8.71	$< 0.001^{***}$	0.15

Table 6.2: *Post hoc* testing in sub-phases (BL vs. AT) separately in each *MIST*-phase. *Note:* $^{*}p < 0.01$, $^{**}p < 0.01$, $^{***}p < 0.001$

Dependant Variable	df_{Num}, df_{Den}	*MIST* phase	*F*	*p*
HR	1, 50	*MIST*1	0.39	0.533
		*MIST*2	5.68	0.021^{*}
		*MIST*3	10.78	$< 0.001^{***}$
pNN50	1, 50	*MIST*1	2.98	0.094
		*MIST*2	0.89	0.353
		*MIST*3	4.42	0.035^{*}
SD1/SD2	1, 50	*MIST*1	5.74	0.017^{*}
		*MIST*2	7.22	0.007^{**}
		*MIST*3	9.16	0.004^{**}

Additionally, the *HR* and *pNN50* showed a significantly increasing latency until both baselines were reached again. This effect was not prominent in *RMSSD* (Table 6.3). Moreover, during *AT* most *HR(V)* measures differed significantly between the *MIST* phases (Table B.1). *Post hoc* testing revealed significant *HR* increases and *HRV* decreases especially between *MIST*1 and *MIST*3 (Table B.2).

Table 6.3: *ANOVA* results (main effect *MIST* phase) of *HR/HRV* changes during *AT* and latency to global baseline and local baselines. *Note:* τ_{glo}: latency until global baseline is reached, τ_{loc}: latency until local baseline is reached, $^{*}p < 0.01$, $^{**}p < 0.01$, $^{***}p < 0.001$.

Dependant Variable	df_{Num}, df_{Den}	*F*	*p*	η_p^2
HR	2, 48	17.67	$< 0.001^{***}$	0.42
HR τ_{glo}	2, 48	4.95	0.011^{**}	0.17
HR τ_{loc}	2, 48	10.81	$< 0.001^{***}$	0.31
RMSSD	2, 48	24.05	$< 0.001^{***}$	0.50
RMSSD τ_{glo}	2, 48	1.33	0.273	0.27
RMSSD τ_{loc}	2, 48	0.63	0.535	0.03
pNN50	2, 48	14.21	$< 0.001^{***}$	0.37
pNN50 τ_{glo}	2, 48	3.48	0.039^{*}	0.13
pNN50 τ_{loc}	2, 48	3.82	0.035^{*}	0.45
SD1/SD2	2, 48	2.94	0.062	0.06

6.1.2 Mood

The stress-inducing effects of the *MIST* are confirmed by the results obtained from the *MDBF* questionnaire. In the *Good-Bad* dimension, a mean decrease of 36.75% with regard to the initial

mood was shown. Moreover, a mean decrease of 33.84% occurred in the *Calm-Nervous* dimension. In the *Awake-Tired* dimension, a lower decrease of 11.30% was shown (Figure 6.2). Nevertheless, all subjects showed a clearly worsened mood after the stress task and the decreases were significant in all three dimensions (Table 6.4).

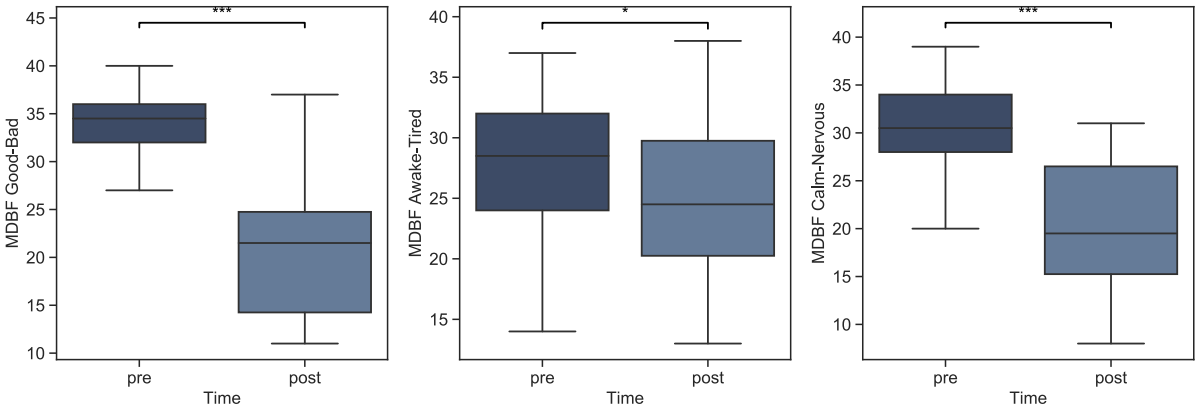

Figure 6.2: Mood decreases induced by the *MIST*. *Note:* $^{*}p < 0.05$, $^{***}p < 0.001$.

Table 6.4: *ANOVA* results of *MDBF* (main effect time). *Note:* $^{*}p < 0.01$, $^{**}p < 0.01$, $^{***}p < 0.001$

Dependant Variable	$\mathrm{df}_{Num}, \mathrm{df}_{Den}$	F	p	η_p^2
MDBF Good-Bad	1, 50	49.50	$< 0.001^{***}$	0.50
MDBF Awake-Tired	1, 50	4.24	0.045^{*}	0.08
MDBF Calm-Nervous	1, 50	36.37	$< 0.001^{***}$	0.42

6.2 Responses to the Cold Face Test

Table 6.5 shows the main findings of the analysis of the *CFT* responses. During the application of the cooling mask, the *HR* and *HR* $\hat{t}_{glo}$ showed decreases in the *CFT* group (Figure 6.3). Additionally, all *HRV* features showed increased values. During all three phases, the differences to the Control group were significant and *post hoc* testing confirmed significantly elevated *HR(V)* values in the *CFT* group (Table B.3).

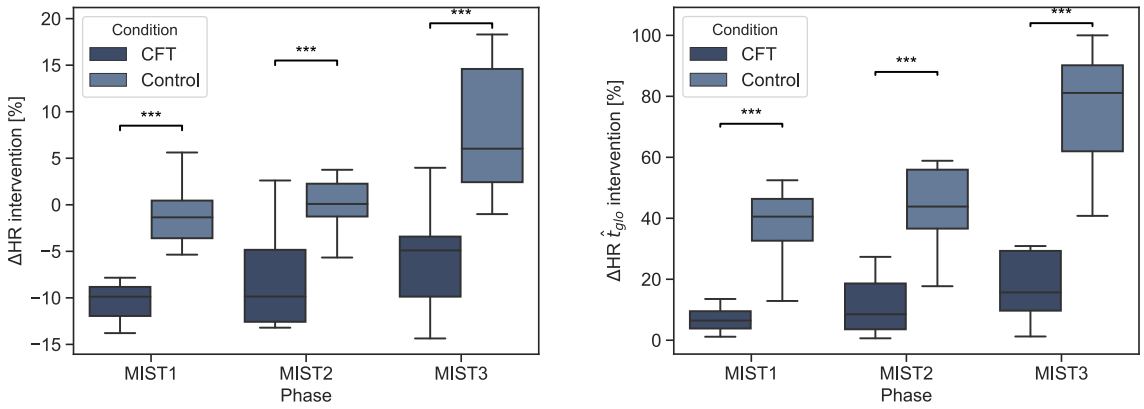

(a) *HR* during Intervention

(b) *HR* $\hat{t}_{glo}$ during Intervention

Figure 6.3: (a) *HR* and (b) *HR* $\hat{t}_{glo}$ during the conduction of the *CFT*. *Note:* *** $p < 0.001$

Table 6.5: *ANOVA* results (main effect condition). *Note:* $\hat{t}_{glo}$: time above global baseline, *LR*: linear regression, $^{*}p < 0.01$, $^{**}p < 0.01$, $^{***}p < 0.001$.

Dependant Variable	df_{Num}, df_{Den}	F	p	η_p^2
HR	1, 24	24.9	$< 0.001^{***}$	0.51
HR LR slope	1, 24	1.73	0.20	0.07
HR $\hat{t}_{glo}$	1, 24	49.27	$< 0.001^{***}$	0.67
RMSSD	1, 24	5.88	0.001^{***}	0.20
RMSSD $\hat{t}_{glo}$	1, 24	8.65	0.006^{**}	0.27
pNN50	1, 24	6.32	$< 0.001^{***}$	0.21
pNN50 $\hat{t}_{glo}$	1, 24	6.12	0.001^{**}	0.28
SD1/SD2	1, 24	11.02	0.003^{**}	0.29

6.3 Distinction between Cold Face Test and Control group

6.3.1 Electrophysiological Measures

General

As shown in Figure 6.4, the *CFT* group showed a decreased *HR* throughout most of the protocol, especially during the Baseline and Intervention sub-phase. Both groups reached the respective peak *HR* values approximately at the same time (at one third of the *AT* sub-phase). However, the *HR* of the *CFT* group decreased slightly right after reaching its peak level during the last *MIST* phase (Figure 6.5). In contrast, the *HR* of the Control group remained at the peak level. Both

groups showed an increasing *HR* during the Feedback interval, but the *HR* of the *CFT* group remained slightly decreased. Similar processes were also prominent in both other *MIST* phases, although they were not that clear (Figure B.1).

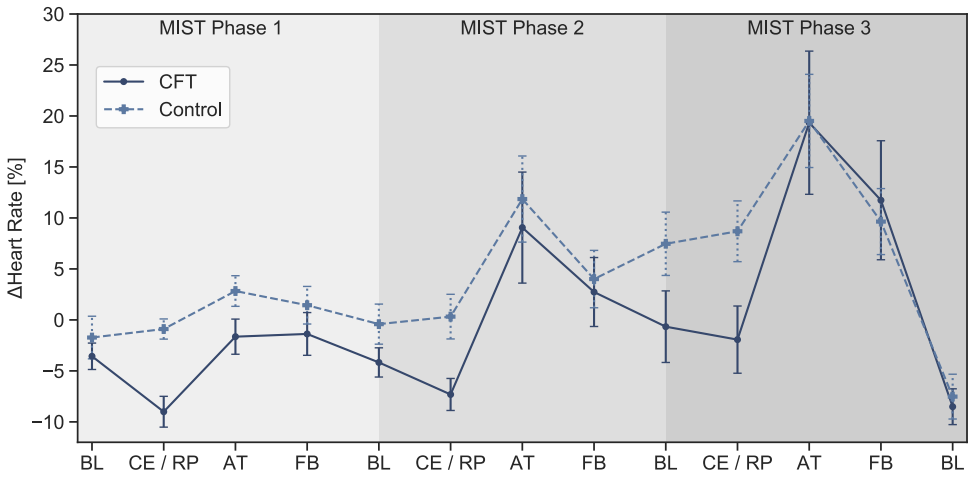

Figure 6.4: *HR* during the conduction of the *MIST*. Each *MIST* phase consisted of a baseline (BL), Cold Exposure Intervention / Resting Period (CE/RP), Arithmetic Tasks (AT) and Feedback (FB) interval. *Note:* Values are depicted as ensemble average and standard error.

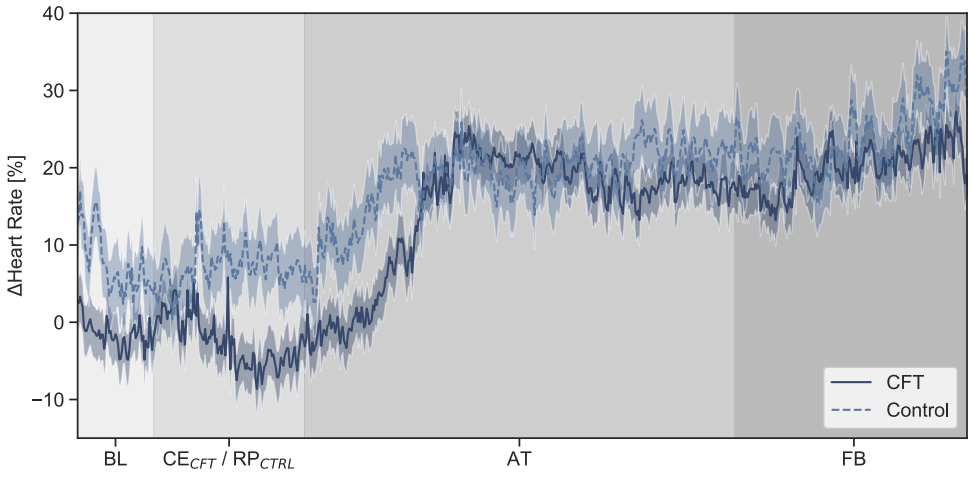

Figure 6.5: *HR* during third *MIST* phase.

Baseline

The baseline *HR* of the *CFT* group was below the baseline *HR* of the Control group throughout the whole *MIST* protocol. Moreover, the baseline *HR* of the *CFT* group remained roughly

constant during the three *MIST* phases, whereas the one of the Control group showed strong increases (Figure 6.6a). *ANOVA* results showed a significant interaction ($p < 0.05$) of condition (*CFT* vs. Control) by phase (Table 6.6). *Post hoc* testing revealed that this effect occurred at the second repetition and remained for the third (Table 6.7). Moreover, the $\hat{t}_{glo}$ measure confirmed the baseline drift of the Control group and the onset after the first *MIST* cycle (Figure 6.6b). Furthermore, the slopes of a linear regression line fitted to the baseline *HR* showed a significantly increased slope for the Control group, whilst the one of the mean of the *CFT* group was close to zero (Control: 4.81, *CFT*: 0.10). The baseline drift was also prominent in the *RMSSD* and *pNN50* measure, but not that clear and not significant. Moreover, the $\hat{t}_{glo}$ measure showed no differences in any *HRV* feature. Generally, the interaction of condition by *MIST* phase is not significant, except for the regression slope of *RMSSD*. Moreover, most *HRV* features showed no significant differences between the conditions (Table 6.6).

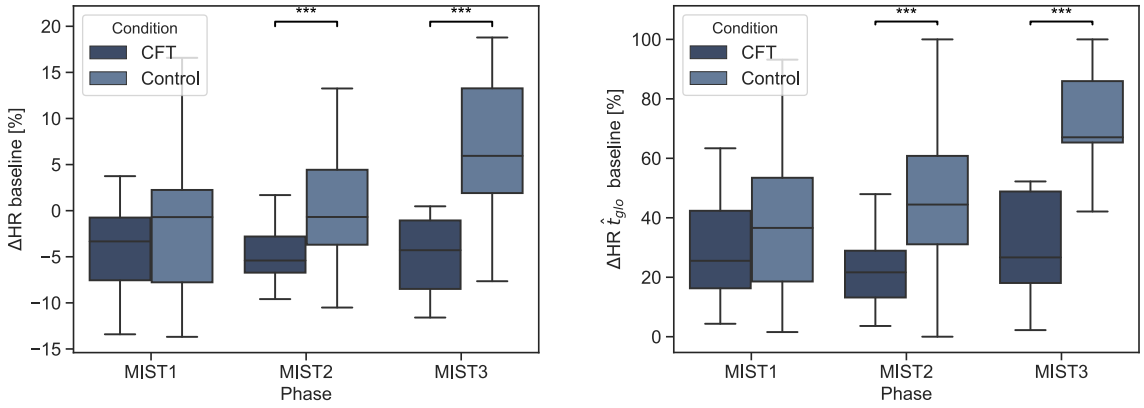

(a) *HR* during baseline

(b) *HR* $\hat{t}_{glo}$ during baseline

Figure 6.6: (a) *HR* and (b) *HR* $\hat{t}_{glo}$ during the one minute baseline interval for the two different conditions. *Note:* *** $p < 0.001$

Arithmetic Tasks

As mentioned in Section 6.1, both groups showed increased values during the stress task. However, the *CFT* group showed slightly decreased *HR* values, but the interaction of condition by *MIST* phase and the main effect of condition were not significant (Table 6.8). The same applied for $\hat{t}_{glo}$ and for all *HRV* features.

Table 6.6: *ANOVA* results during Baseline sub-phase (interaction condition by *MIST* phase). *Note:* LR: linear regression, ^{c} annotates the main effect condition, $^{*}p < 0.01$, $^{**}p < 0.01$, $^{***}p < 0.001$.

Dependant Variable	df_{Num}, df_{Den}	F	p	η_p^2
HR	2, 48	5.17	0.006^{**}	0.18
HR $\hat{t}_{glo}$	2, 48	3.32	0.045^{*}	0.12
HR LR slope	1, 24	11.35	$< 0.001^{***}$	0.32
RMSSD ^{c}	1, 24	2.51	0.126	0.20
RMSSD $\hat{t}_{glo}$ ^{c}	1, 24	0.258	0.616	0.01
RMSSD LR slope	1, 24	5.80	0.016^{*}	0.20
pNN50 ^{c}	1, 24	2.05	0.165	0.21
pNN50 $\hat{t}_{glo}$ ^{c}	1, 24	0.47	0.63	0.27
SD1/SD2	2, 48	0.17	0.84	0.01

Table 6.7: *Post hoc* testing during Baseline separately in each *MIST* phase. *Note:* $^{*}p < 0.01$, $^{**}p < 0.01$, $^{***}p < 0.001$

Dependant Variable	df_{Num}, df_{Den}	*MIST* phase	*F*	*p*
HR	1, 24	*MIST*1	1.23	0.279
		*MIST*2	6.43	0.011^{**}
		*MIST*3	11.18	$< 0.001^{***}$
HR $\hat{t}_{glo}$	1, 24	*MIST*1	0.99	0.331
		*MIST*2	6.10	0.014^{*}
		*MIST*3	13.67	$< 0.001^{***}$

Table 6.8: *ANOVA* results during the Arithmetic Tasks sub-phase (main effect condition).

Dependant Variable	df_{Num}	df_{Den}	F	p	η_p^2
HR	1	24	1.11	0.302	0.04
HR $\hat{t}_{glo}$	1	24	3.94	0.059	0.14
RMSSD	1	24	2.89	0.102	0.10
RMSSD $\hat{t}_{glo}$	1	24	3.30	0.082	0.12
pNN50	1	24	2.14	0.157	0.08
pNN50 $\hat{t}_{glo}$	1	24	2.46	0.130	0.09
SD1/SD2	1	24	2.22	0.157	0.09

6.3.2 Cortisol

The *CFT* and the Control group showed similar cortisol responses (Figure 6.7a). Moreover, the initial values of both groups did not differ considerably, even though the Control group showed slightly decreased values. Furthermore, both groups reached their post-stress peak level 20 minutes

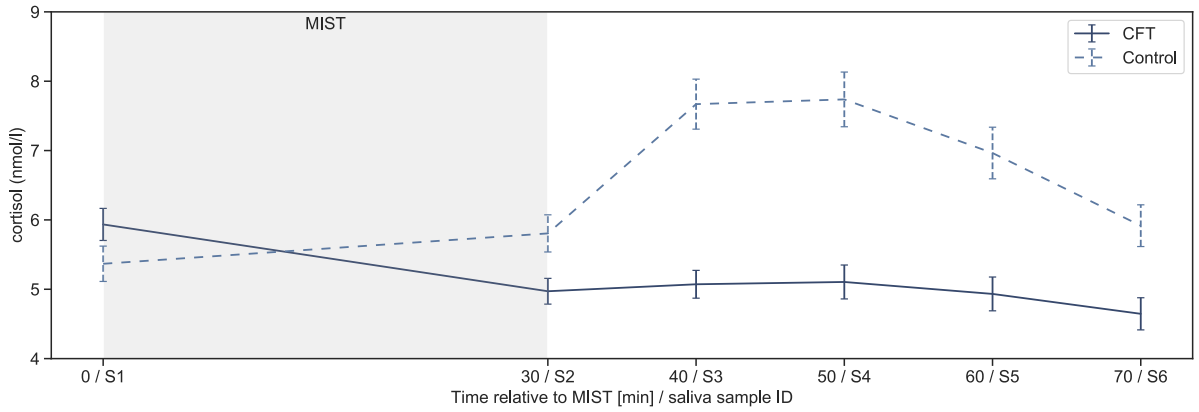

(a) Cortisol concentration

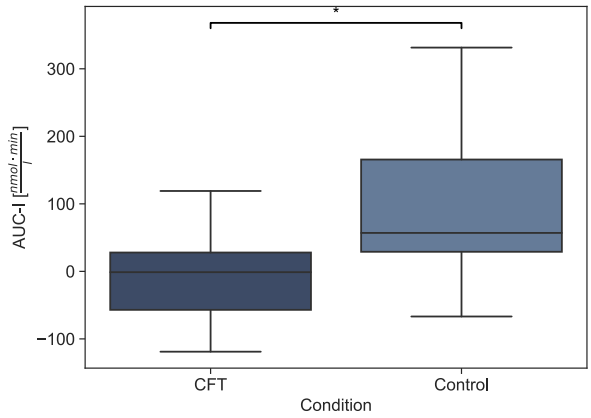

(b) *AUC-I*

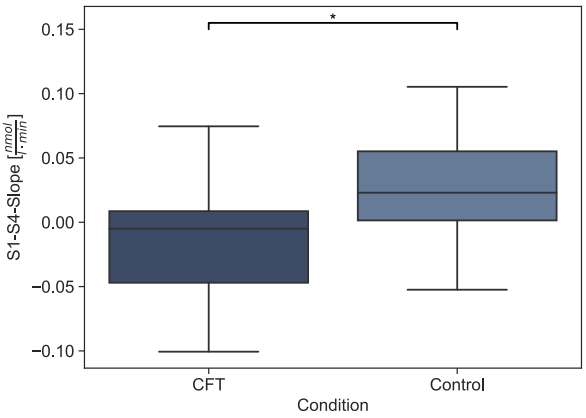

(c) S1-S4-Slope

Figure 6.7: (a) Cortisol levels; (b + c) cortisol-derived features. Note: * $p < 0.05$; values in (a) are displayed as mean and standard error.

after the end of the *MIST*. However, the cortisol response of the *CFT* was clearly weakened. In fact, the mean relative increase from the pre-*MIST* saliva sample (S1) to the peak level (S4) was clearly higher in the Control group (*CFT* group: -14.52%, Control group: 42.89%). The mean peak concentration of the *CFT* group was actually below its initial value, whilst the Control group showed a strong increase. Additionally, the cortisol level of the *CFT* group decreased during the *MIST* conduction, whilst the Control group showed a rather constant level.

In Table 6.9, the most important findings are displayed. The *CFT* group showed significantly decreased cortisol levels throughout the whole study protocol. Nevertheless, *post hoc* testing in each condition separately did not reveal significant differences over time (main effect of time: Control: F(1, 24) = 1.81, p = 0.191, *CFT*: F(1, 24) = 0.43, p = 0.518). However, the *CFT* group showed significantly decreased *AUC-I* (Figure 6.7b), post-*MIST AUC-I* (*AUC-I*$_{pm}$) and slope

between S1 and S4 (Figure 6.7c). Additionally, the *CFT* group showed significantly decreased variation, shown by a significantly decreased standard deviation in the cortisol levels, throughout the whole protocol. In contrast, there were no significant differences between *CFT* and Control group in *AUC-G* and post-*MIST AUC-G* (*AUC-G*$_{pm}$).

Table 6.9: *ANOVA* results of the cortisol analysis (main effect condition). *Note:* ^{c*t}: interaction of condition and time, *STD*: standard deviation; $^{*}p < 0.05$, $_{pm}$: post-*MIST*, $^{**}p < 0.01$, $^{***}p < 0.001$.

Dependant Variable	df$_{Num}$	df$_{Den}$	F	p	η_p^2
cortisol ^{c*t}	5	120	3.84	0.003**	0.14
cortisol STD	1	10	15.65	$< 0.001^{***}$	0.61
AUC-I	1	24	5.03	0.034*	0.17
AUC-I$_{pm}$	1	24	4.85	0.037*	0.17
S1-S4-Slope	1	24	6.42	0.038*	0.21
AUC-G	1	24	0.484	0.365	0.03
AUC-G$_{pm}$	1	24	2.11	0.160	0.08
S1-S4 Difference	1	24	4.23	0.081	0.15

6.3.3 Mood

The *CFT* group showed slightly decreased mood worsening in the *Awake-Tired* dimension (see Figure 6.8). There were no significant differences between the *CFT* and Control group (Table 6.10), even though the *CFT* group showed slightly decreased mood worsening (Figure 6.8).

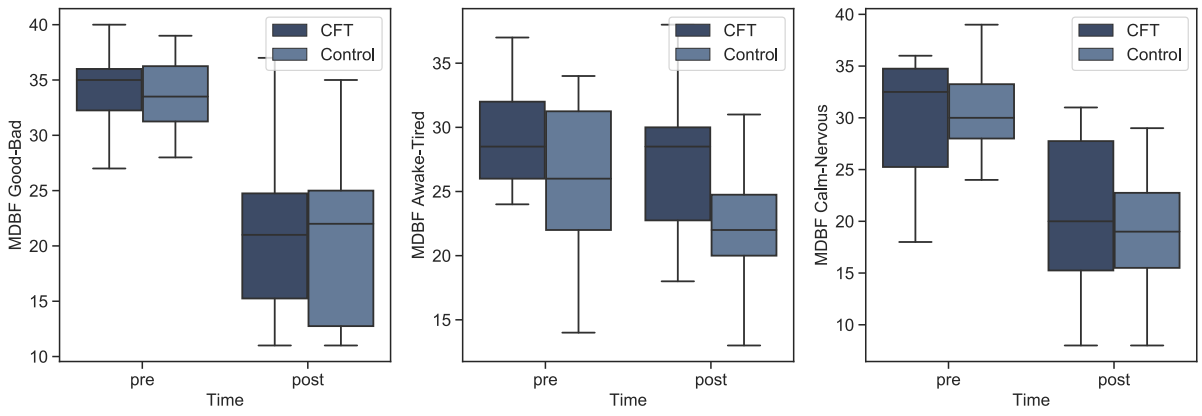

Figure 6.8: Results of *MDBF* Questionnaire.

Table 6.10: *ANOVA* results of the mood analysis (main effect condition).

Dependant Variable	df_{Num}	df_{Den}	F	p	η_p^2
Good-Bad	1	24	3.23	0.80	0.00
Awake-Tired	1	24	3.85	0.06	0.14
Calm-Nervous	1	24	0.00	0.94	0.00

6.3.4 Differences in Cold Face Test Responder Types

Electrophysiological Measures

Based on La Marca et al. [Mar11], a median split based on the *latency to peak bradycardia* (τ_{pb}) was performed with the *CFT* group. Thus, the two resulting responder groups consisted of six and seven subjects.

In general, the *Slow Responder (SR)* showed increased *HRV* values during all phases. Compared to *Fast Responder (FR)* and Control group, the *SR* group showed significantly increased *RMSSD* values during the *CFT* (main effect of responder types: F(2, 25) = 10.78, $p < 0.001$, $\eta_p^2 = 0.45$) and Arithmetic Tasks (main effect of responder types: F(2, 25) = 8.57, $p < 0.001$, $\eta_p^2 = 0.32$), as revealed by *post hoc* testing (Figure 6.9).

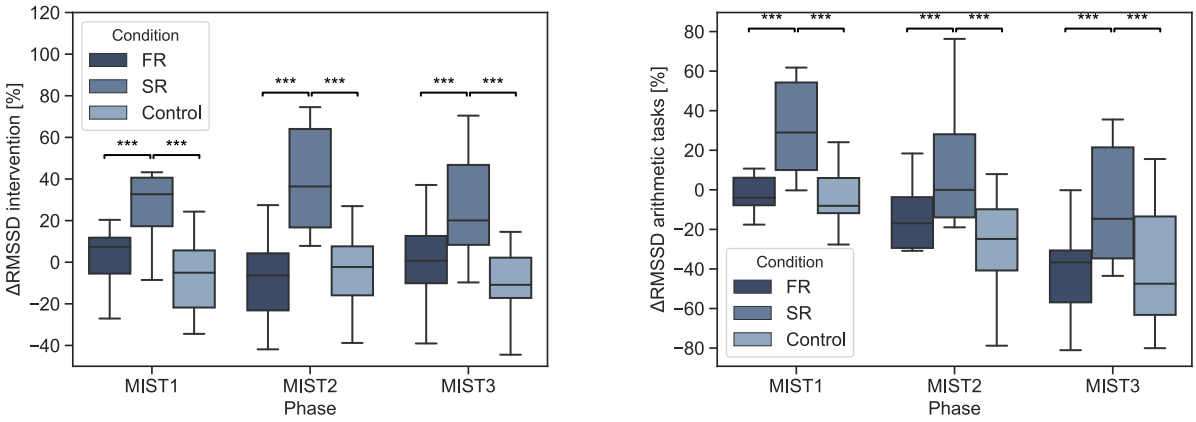

(a) *RMSSD* during Intervention

(b) *RMSSD* during *AT*

Figure 6.9: *RMSSD* over the three *MIST* phases. *Note:* $^{***}p < 0.001$.

Cortisol

The *SR* group showed lower cortisol concentrations (Figure 6.10). In fact, the interaction of Responder Types by sample ID was significant (F(10, 115) = 1.93, p = 0.048, $\eta_p^2 = 0.14$). *Post hoc*

testing revealed significantly decreased cortisol levels for the *SR* group compared to the Control group ($p < 0.001$), but not to the *FR* group ($p = 0.059$). Moreover, *FR* did not show significantly decreased cortisol values compared to the Control group ($p = 0.69$). In contrast to that, the *FR* group showed decreased areas under the curve, differences and slopes between S1 and S4, but neither of these measures did differ significantly ($F(2, 23) < 1.34$, $p > 0.110$, $\eta_p^2 < 0.18$).

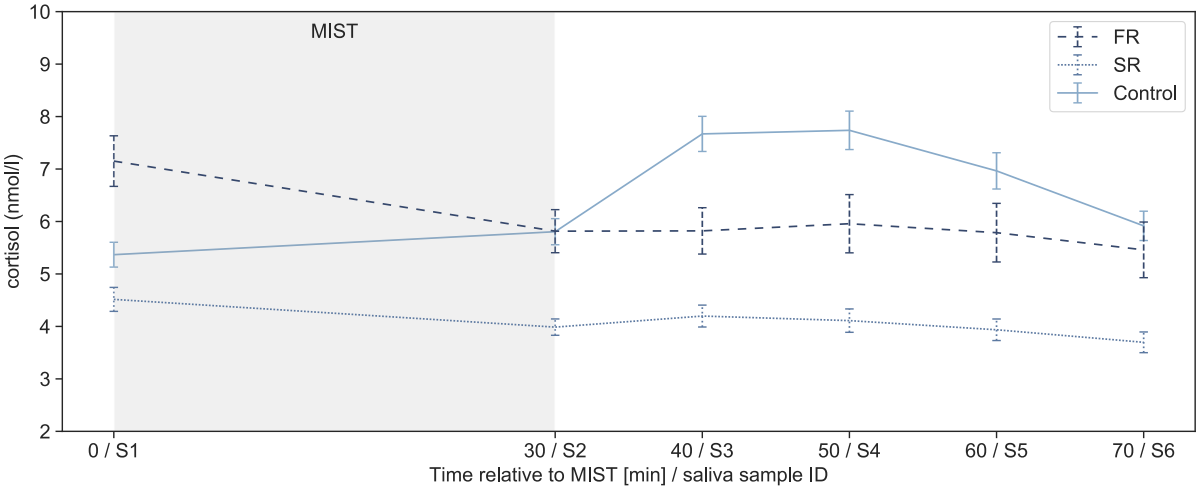

Figure 6.10: Cortisol process of the *CFT*-subgroups and Control group. *Note:* Values are displayed as ensemble average and standard error

Mood

In accordance to the decreased cortisol concentrations in the *SR* group, the mood worsening in the *SR* group was also decreased. However, these differences were not significant in neither of the three mood-scales (main effect responder types: $F(1, 23) < 1.96$, $p > 0.16$, $\eta_p^2 < 0.16$).

Chapter 7

Discussion

The main objective of the present study was to assess whether the *CFT*-induced stimulation prior to the occurrence of a stressor diminishes the stress response. Along with this hypothesis, the inhibitory vagal effect on the *HPA* axis was investigated. In this context, the obtained results regarding the stress induction by the *MIST*, *CFT*-induced parasympathetic stimulation, and the distinction between *CFT* and Control group are discussed below. Last, the findings of La Marca et al. are transferred to the present study and discussed [Mar11].

The present study is compromised by two general limitations. First, the majority of the subjects were females. In general, females show decreased cortisol responses to acute psychological stress [Ste16]. Moreover, the use of oral contraceptives was no exclusion criteria. Oral contraceptives however, attenuate the cortisol response to a stressor [Kir95]. Additionally, cortisol concentrations can be affected by several biological factors such as, for instance, weight, age, and sex [Ber87]. Nevertheless, both groups were balanced with regard to sex, age, and weight. Thus, these factors should not affect the present study.

Furthermore, the study was conducted between 11:00 a.m. and 5:30 p.m. As the curve of the diurnal cortisol concentrations reaches a flatter area between 1:30 p.m. and 4:15 p.m. it is recommended to conduct stress studies only within this time slot. However, the slope of the diurnal cortisol concentration decreases with the time after wakening [Ski11]. To diminish the effect of decreasing cortisol levels during the stress task due to the diurnal rhythm, subjects were asked to wake up at least three hours before the study so the cortisol curve was already flattened.

7.1 Responses to the Stress Task

The findings obtained in this study reproduce those of prior investigations (e.g. Dedovic et al. [Ded05]): an increase in cortisol concentrations as a response to the *MIST*. Thus, a successful stress-induced stimulation of the *HPA* axis is indicated. This is further supported by a significantly ($p = 0.048$) increased *HR* during the Arithmetic Tasks compared to the resting *HR*. Moreover, all *HRV* features showed decreased levels during the Arithmetic Tasks.
Besides, the *MDBF* scores showed a significant (Good-Bad: $p < 0.001$, Awake-Tired: $p = 0.045$, Calm-Nervous: $p < 0.001$) worsening in mood induced by the *MIST*. Thus, the subjective stress perception also showed an increase in perceived stress as a response to the stress task.
The obtained results not only showed an increase in stress, but the increase of the induced stress throughout the single *MIST* cycles. The mean *HR* level during the three repetitions of the *AT* showed a constant and significant ($p < 0.001$) increase indicating an effective inhibition of the *PSNS*. Accordingly, *HR* τ_{glo} decreased significantly ($p = 0.011$) between the phases. This trend is also prominent in all *HRV* features and shown by the significantly increasing *pNN50* latency to both baselines ($p < 0.040$) indicating that subjects needed more time to recover from the stress over the course of the procedure. Thus, the (increasing) stress induction by the *MIST* is clearly reproduced in the present study.

7.2 Responses to the Cold Face Test

The *CFT* clearly induced vagal activity and thus parasympathetic activity. This is shown by a significantly decreased *HR* and $\hat{t}_{glo}$ ($p < 0.001$) indicating a *CFT*-induced bradycardia. Moreover, the significantly increased *HRV* features ($p < 0.007$), along with the respective increased times above baseline, support the successful parasympathetic stimulation in the *CFT* group during the Intervention phases.
Remarkably, the *HR* $\hat{t}_{glo}$ of the *CFT* was below 50% during all three *CFT* applications. The same applies for the *HRV* features. However, both groups showed similar *HR* increases during the Intervention sub-phase over the three *MIST* phases, indicating that the *CFT* is weakened over time. This trend is illustrated by the linear regression through the mean heart rates during Intervention, indicating positive regression slopes for both groups. Nevertheless, the regression slope of the *CFT* group is lower as the one of the Control group. During the last *MIST* phase the *CFT* group showed a mean *HR* decrease of about 5%. Along with the fact that the *CFT* group generally shows a significantly decreased *HR* during Intervention ($p < 0.001$), it can be stated that the *CFT*

induces *HR* decreases even after a stress task and in the face of a reoccurring stressor. Thus, the *CFT* induces parasympathetic activity regardless of the prior enhancement of the *SNS* and a possible anticipatory stress reaction. Based on current knowledge, this is the first study that showed this.

7.3 Distinction between Cold Face Test and Control Group

7.3.1 Electrophysiological Measures

The most reliable *ECG*-related markers of stress level are the *HR*, Low/High Frequency (LF/HF) ratio, *RMSSD*, and *pNN50* [Kim18]. According to Malik et al., intervals with a duration of at least five minutes should be recorded if *HRV* frequency analysis is consulted [Mal96]. Thus, it was not applied in this thesis, as most of the intervals (except for the rest and recovery phase) were shorter than five minutes. However, three of the four named most reliable *HRV* features were computed in this thesis.

As mentioned before, *RSA* was excluded from further analysis. Especially during the Arithmetic Task session, subjects moved a lot and bent over the desk. Hence, the sensor detached from the thorax and the correct recording of the thorax movements could not be ensured anymore. However, *RSA* is rather unreliable anyway, as it alters with the respiration frequency and tidal volume and must therefore be interpreted with caution [Gro04][Kim18].

The *CFT* group showed decreased *HR* values throughout the whole study, but differences to the Control group were only in parts significant. In fact, none of the *HR(V)* features showed significant differences between the two groups during the Arithmetic Tasks ($p > 0.080$). Thus, the *CFT*-induced enhanced activity of the *PSNS* during the prior intervention is abolished by the dominating sympathetic activation during the actual stress task.

Unlike during the Arithmetic Tasks, the *CFT* group showed significantly ($p = 0.006$) decreased baseline heart rate starting with the second *MIST* phase. The same applied for $\hat{t}_{glo}$. Thus, the Control group showed decreased *HR* features starting after the first occurrence of the stressor. Since both groups showed a similar baseline *HR* during the first *MIST* phase, the drift of the Control group indicates difficulties to return to the initial resting heart rate. Additionally, the Control group showed decreasing *RMSSD*, *RMSSD* $\hat{t}_{glo}$, *pNN50*, and *pNN50* $\hat{t}_{glo}$ baseline values. Furthermore, the Control group showed a significantly higher regression slope for *HR* and *RMSSD* ($p < 0.001$) and thus a significantly stronger *HR* baseline increase or rather *RMSSD* baseline decrease throughout the three *MIST* phases. All of the above findings count in favor of the hypothesis that the Control group struggles to return to their respective resting heart rate after the

end of the stressor. Only in the SD1/SD2 ratio there are no significant differences between both groups. However, the SD1/SD2 ratio does not count to the most reliable *HRV* features and thus it should not be necessarily taken into closer consideration especially as all other *HR(V)* features disagree with it [Kim18].
Remarkably, the differences between the groups occur during all baseline intervals, but not during the stress periods. Thus, it seems like the *CFT*-induced parasympathetic activation is present during the stress phases but is rather put in the background by the dominating sympathetic activation during the Arithmetic Tasks sub-phase. Once the sympathetic stimulus is withdrawn, i.e. the Arithmetic Tasks and Feedback intervals are over, the *CFT* group recovers to the initial state due to the maintained activity of the *PSNS* .

7.3.2 Cortisol

The lack of significant differences in the *AUC-G*, *AUC-*G_{pm}, and the cortisol difference between S1 and S4 suggests that the *CFT*-induced effects do not inhibit the *HPA* axis activity.
In contrast to that and in accordance to the *HR(V)* findings, the *AUC-I* (p = 0.034), *AUC-*I_{pm} (p = 0.037), and slope between S1 and S4 (p = 0.038) show significantly decreased values for the *CFT* group. Therefore, the results from the cortisol analysis undermine the hypothesis that the *CFT* successfully interferes with the stress pathways by parasympathetic inhibition of the *HPA* axis.
Remarkably, the *AUC-G* features did not differ significantly, whilst the *AUC-I* ones showed significant differences. This is probably due to the fact that the *AUC-G* illustrates the absolute cortisol output, whilst *AUC-I* must be rather interpreted as changes relative to the initial level [Pru03]. Therefore, the *AUC-I* represents a better measure for the changes induced by the *MIST*. This means that the Control group showed significantly increased cortisol concentrations with respect to the initial value, whilst the *CFT* group did only show a weak cortisol response to the occurred stressors.
In addition to that, the cortisol response of the *CFT* group was decreasing throughout the whole procedure, whilst the Control group showed mostly increasing values. Moreover, the cortisol levels of the *CFT* group after the *MIST* were significantly decreased (p = 0.003). Hence, the application of the *CFT* prior to the stress task did actually decrease the amount of cortisol that is secreted due to the stress task. Consequently, these findings show the inhibitory effect of the *CFT*-induced vagal stimulation on the *HPA* axis.

7.3.3 Mood

There were no significant differences in all three mood scales, although the *CFT* group showed rather decreased worsening in mood. This is in fact surprising as the electrophysiological and cortisol-related features confirm differences between both groups. Moreover, Ingjaldsson et al. actually found that *HRV* is negatively correlated with negative mood and positively correlated with positive mood [Ing03]. However, the present findings do not support their findings. Even though it seems like the *CFT* group showed better mood, no significant differences between the groups were revealed. This may result from the fact that the *CFT* directly influences the *ANS* and *HPA* axis. In contrast, mood results from the interplay of various biological players and is thus only indirectly affected by the *ANS* and the *HPA* axis. Hence, the mood response may be weakened. However, larger subject populations may enhance the differences and help to cope with this effect.

7.4 Distinction between Responder Types and Control

The results presented in Section 6.3.4 suggest that the *SR* group showed a lower stress response than the Control group *and* the *FR* group. In fact, the *SR* showed significantly higher *RMSSD* values during the Arithmetic Tasks ($p < 0.001$). The *FR* showed *RMSSD* values similar to the Control group. Moreover, the *SR* group showed significantly higher *RMSSD* values during Intervention than the *FR* group ($p < 0.001$). Latter actually showed *RMSSD* values during Intervention that were once again similar to the Control group. Thus, the *SR* showed higher responses to the *CFT*. This may explain the reduced *RMSSD* decrease in the *CFT* group during the actual stress task.

In accordance to the *RMSSD* values, the *SR* showed decreased worsening in mood, but these differences were not significant ($p > 0.16$).

Yet, these findings are also in line with the obtained cortisol results. Here, the *SR* group showed significantly lower concentrations than the Control group ($p < 0.001$), but not significantly lower than the *FR* group ($p = 0.059$). Remarkably, the *FR* showed a largely biased cortisol response that most likely caused the differences between *SR* and *FR*. In fact, this is confirmed by a decreased post-*MIST* cortisol response in the *FR* group. Additionally, a slightly decreased *AUC-*I_{pm} and a slightly lower S1-S4-Slope further confirm this theory. However, none of these differences between the two responder types were significant ($p > 0.11$).

Nevertheless, these differences may result from the fact that a longer latency to peak bradycardia may be linked to longer cold-face stimulation. Thus, the vagus nerve is stimulated longer and con-

sequently reaches its maximum responsiveness later. Hence, a longer latency to peak bradycardia may be linked to a longer lasting vagal stimulation and thus a longer lasting stimulation of the *PSNS*.

The just mentioned results contradict the hypothesis of La Marca et al. that subjects with a low latency to peak bradycardia have lower worsening in mood and lower cortisol responses [Mar11]. However, La Marca et al. used a different study protocol. Moreover, in the present study, the responder groups consisted of only 6 subjects for the *FR* and 7 for the *SR* group, respectively. Thus, these findings should rather be seen as an exploratory approach in transferring the findings of La Marca et al. on the present setup and the magnitude of these findings should be critically assessed.

Chapter 8

Conclusion and Outlook

The major research goal of this thesis was the investigation of the suitability of the *CFT* as an intervention method for reducing an acute stress response by inhibiting the *SNS* and the *HPA* axis through parasympathetic activation. For this purpose, the *MIST* was conducted with 28 healthy subjects. In the *CFT* group, results showed a decreased cortisol response to the exposed stressor. Even though no significant differences occurred during the actual stress task, the *CFT*-induced activity of the *PSNS* significantly accelerated the recovery from the previous stressor, indicated by a significantly decreased *HR* baseline drift. Last, the present study showed that the *CFT* induced bradycardia and thus parasympathetic activity even in the light of varying and intense acute stress exposure. In conclusion, the present study confirmed the suitability of the *CFT* as a measure to inhibit the *HPA* axis activity and, in parts, the *SNS*, thus resulting in an inhibition of the stress response.

Based on further research and the analysis of amylase, that has yet to be performed, the *CFT*-induced inhibition of the acute stress response can be assessed even further.

Additionally, the distinction between people with a low and high *CFT* reactivity or between people with a weak and strong *CFT* response should be assessed with larger subject populations.

A further approach would be the investigation of the *CFT*-induced effects in the light of different kinds of stress. Thus, the previous hypothesis of maintained parasympathetic stimulation could be further evaluated.

Another interesting topic for further work could be the exploration of long-term effects of the *CFT* on the regulation of the stress system. In this context, maybe even therapeutic aspects could be investigated such as, for instance, the effect on patients with a preexisting deregulated stress system, the prevention of said or the effect of the *CFT* on chronic stress.

Appendix A

Patents

A.1 Method and apparatus for the use of a network system for biofeedback stress reduction

Publication Number	US20020083122A1
Date of Publication	Jun. 27, 2002
Inventors	Marc S. Lemchen
Assignee	Lemchen Marc S.
Abstract	A system for reducing stress comprises a computer which operates a software program. The program may be run locally or from a remote server via the world wide web. A user inputs information into the computer relating to his or her body, lifestyle, work schedule. A sensor may be attached to the user and coupled to the computer to receive autonomic signals from the user. The computer executes a series of stress reducing exercises which the user is directed to perform. The system monitors and records the user's compliance, or lack thereof. The system then adjusts the stress reducing exercises based the user's performance.

A.2 Rhythmic biofeedback technique

Publication Number	US5007430A
Date of Publication	Apr. 16, 1991
Inventors	Irving I. Dardik
Assignee	Lifewaves International Inc
Abstract	A rhythmic biofeedback technique for inducing relaxation to counteract the adverse physiological and psychological effects of chronic stress on an individual. In this technique, the heart beat of the individual being treated is continuously monitored and the prevailing rate is displayed to him as he undergoes a rhythmic conditioning session constituted by successive exercise-relaxation cycles extending for a predetermined period. In the course of each cycle, the individual is required to raise his level of exertion, as indicated by his perceived heart beat rate, to a peak representing an established safe upper limit, following which he is required to decrease his exertion until he reaches a lower limit at which a recovery relaxation response takes place. The upper and lower limits are determined by the individual's existing capacity for exercise and define his target heart rate zone.

Appendix B

Additional Figures and Tables

Table B.1: *ANOVA* results of increasing *MIST*-induced stress levels (main effect phase). Note: df_{Num}: degrees of freedom of the numerator, df_{Den}: degrees of freedom of the denumerator; ˆ : Greenhouse-Geiger corrected p-values, $\hat{t}_{glo}$: time above global baseline, $^{***}p < 0.001$.

Dependant Variable	df_{Num}, df_{Den}	*F*	*p*	η_p^2
HR during intervention	2, 48	16.72	< 0.001ˆ ***	0.41
HR $\hat{t}_{glo}$ intervention	2, 48	13.96	$< 0.001^{***}$	0.37
HR AT	2, 48	17.67	$< 0.001^{***}$	0.42
HR $\hat{t}_{glo}$ *AT*	2, 48	39.00	$< 0.001^{***}$	0.62
RMSSD AT	2, 48	24.05	$< 0.001^{***}$	0.50
RMSSD $\hat{t}_{glo}$ *AT*	2, 48	23.25	$< 0.001^{***}$	0.49
pNN50 AT	2, 48	14.21	< 0.001ˆ ***	0.37
pNN50 $\hat{t}_{glo}$ *AT*	2, 48	32.27	$< 0.001^{***}$	0.57
SD1/SD2 *AT*	2, 48	2.94	0.059	0.11

Table B.2: *Post hoc* testing results during *AT* (between: *MIST* phases). Note: df_{Num} stands for the degrees of freedom of the numerator, while df_{Den} stands for the degrees of freedom of the denumerator. $\hat{t}_{glo}$: time above global baseline, $^{*}p < 0.05$, $^{***}p < 0.001$.

Dependant Variable	*MIST* phase	*T*	*p*
HR	*MIST*1 - *MIST*2	-2.31	0.056
	*MIST*1 - *MIST*3	-4.07	$< 0.001^{***}$
	*MIST*2 - *MIST*3	-1.76	0.185
HR τ_{glo}	*MIST*1 - *MIST*2	-3.35	0.083
	*MIST*1 - *MIST*3	-5.42	$< 0.039^{*}$
	*MIST*2 - *MIST*3	-2.08	0.900
HR τ_{loc}	*MIST*1 - *MIST*2	-3.70	$< 0.001^{***}$
	*MIST*1 - *MIST*3	-4.16	0.041^{*}
	*MIST*2 - *MIST*3	-0.46	0.173
RMSSD	*MIST*1 - *MIST*2	2.51	0.033^{*}
	*MIST*1 - *MIST*3	4.24	$< 0.001^{***}$
	*MIST*2 - *MIST*3	1.73	0.196
pNN50	*MIST*1 - *MIST*2	1.36	0.363
	*MIST*1 - *MIST*3	2.88	0.011^{*}
	*MIST*2 - *MIST*3	1.52	0.282
pNN50 τ_{glo}	*MIST*1 - *MIST*2	2.72	0.323
	*MIST*1 - *MIST*3	4.59	0.063
	*MIST*2 - *MIST*3	1.87	0.674
pNN50 τ_{loc}	*MIST*1 - *MIST*2	2.90	0.028^{*}
	*MIST*1 - *MIST*3	3.72	0.169
	*MIST*2 - *MIST*3	0.67	0.701

Table B.3: *Post hoc* results testing (between: conditions) during sub-phase Intervention. *Note:* $^{**}p < 0.01$, $^{***}p < 0.001$

Dependant Variable	*T*	*p*
HR	-6.24	0.001^{***}
HR $\hat{t}_{glo}$	-7.46	0.001^{***}
RMSSD	3.32	0.001^{***}
RMSSD $\hat{t}_{glo}$	4.20	0.001^{***}
pNN50	3.25	0.001^{**}
pNN50 $\hat{t}_{glo}$	4.28	0.001^{***}
SD1/SD2	3.89	0.001^{***}

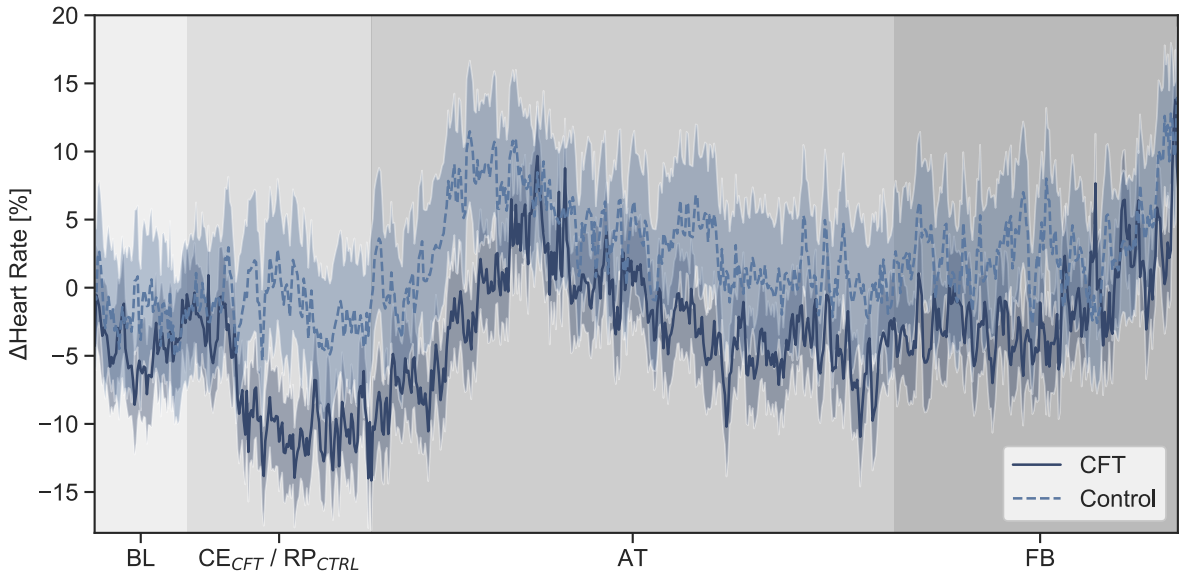

(a) *HR* during first *MIST* phase.

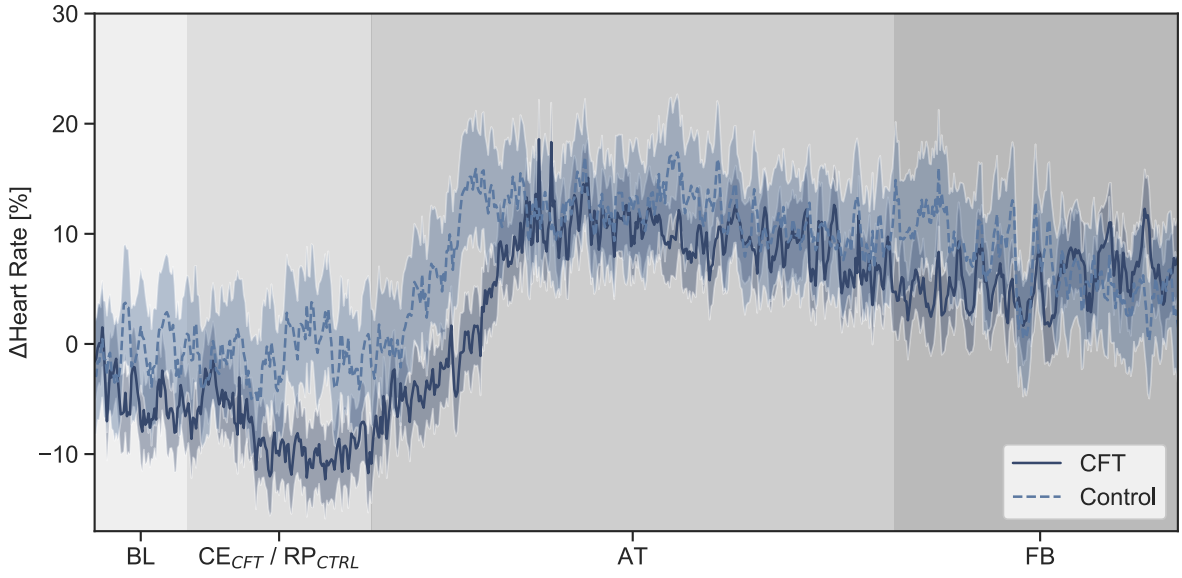

(b) *HR* during second *MIST* phase.

Figure B.1: Source of Heart Rate (displayed as *HR* increase relative to global baseline) of both groups during *MIST* phases 1 and 2.

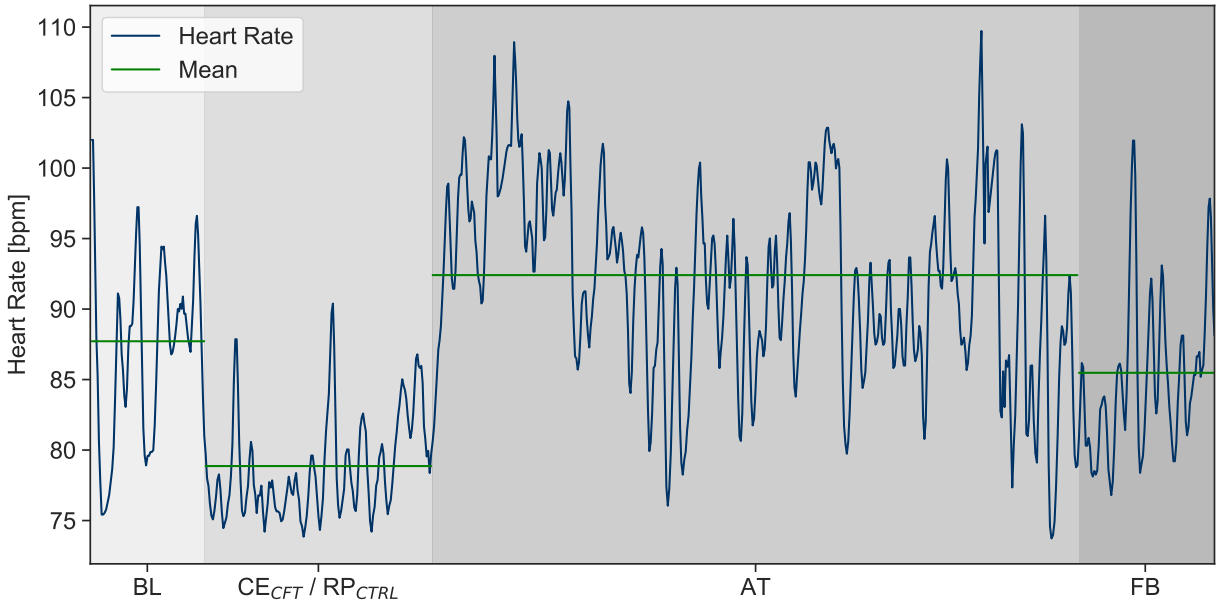

(a) *HR* during the third *MIST* cycle.

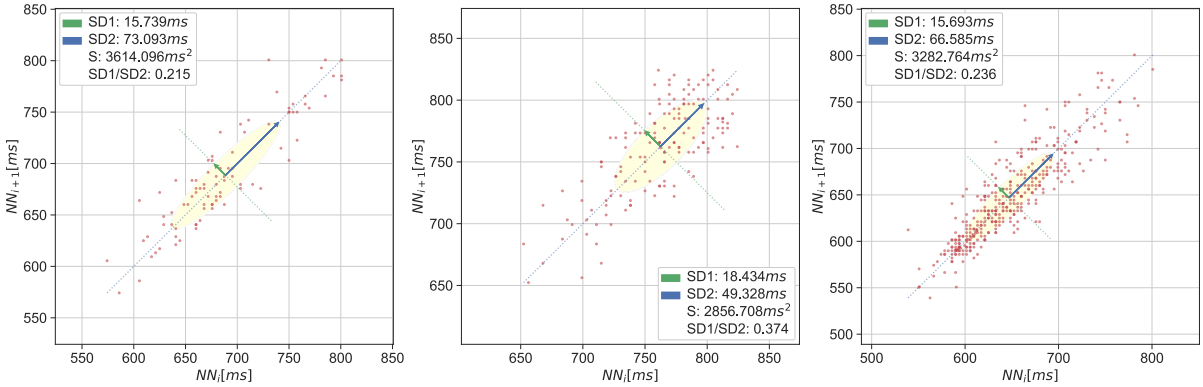

(b) Baseline **(c)** Intervention **(d)** Arithmetic Tasks

Figure B.2: *HR* and Poincaré Plots during the conduction of the *CFT* and the successive stress task. The lower the *HR* is, the wider the point cloud spreads.

Glossary

ACTH Adrenocorticotropic Hormone

ADS-L German version of the Center for Epidemiologic Studies Depression Scale

ANOVA Analysis of Variance

ANS Autonomous Nervous System

AT Arithmetic Tasks

AUC-G Area under the curve with respect to ground

AUC-I Area under the curve with respect to increase

CFT Cold Face Test

CRH Corticotrophin-Releasing Hormone

DR Diving Response

ECG Electrocardiogram

FD Familial dysautonomia

FR Fast Responder

HPA Hypothalamus-Pituitary-Adrenal

HR Heart Rate

HRV Heart Rate Variability

MBSR Mindfulness-based stress reduction

MDBF German version of the Mulitdimensional Mood State Questionnaire

MIST Montreal Imaging Stress Task

MRI Magnetic Resonance Imaging

PET Positron Emission Tomography

pNN50 Percentage Of Successive RR-Intervals differing more than 50 ms

PSNS Parasympathetic Nervous System

RMSSD Root Mean Square Of Successive Differences

RR50 Number Of Successive RR-Intervals differing more than 50 ms

RSA Respiratory Sinus Arrhythmia

SNS Sympathetic Nervous System

SR Slow Responder

TMCT Trier Mental Challenge Test

TSST Trier Social Stress Test

List of Figures

2.1 Illustration of the stress response creation 6
2.2 Cranial Nerves 10
2.3 DR and CFT 11

4.1 Lead II ECG 20
4.2 Android application for the sensor 21
4.3 Detected R-Peaks 23
4.4 HR during CFT 24
4.5 RMSSD during the CFT 25
4.6 pNN50 during the CFT 25
4.7 RSA Determination 27
4.8 Poincaré Plot 28
4.9 Cortisol-derived Features 30

5.1 Computer interface of the MIST 32
5.2 HR during the pre-study 34
5.3 Study protocol 35

6.1 HR during the MIST 40
6.2 MIST-induced mood worsening 42
6.3 HR and HR $\hat{t}_{glo}$ during CFT 43
6.4 HR during the conduction of the MIST 44
6.5 HR during third MIST phase 44
6.6 HR and HR $\hat{t}_{glo}$ baseline drift 45
6.7 Cortisol-derived features during MIST 47
6.8 Mood Decrease between groups 48
6.9 RMSSD between Responder Types 49

6.10 Cortisol process in Responder Types 50

B.1 HR process during MIST 63
B.2 Poincaré Plot and its connection to the HR 64

List of Tables

4.1 HR(V) Features 22

5.1 Pre-Study Results 34
5.2 Demographic study data 35
5.3 Saliva samples times 36
5.4 Feature-derived measures 37

6.1 Anova results of HRV analysis 40
6.2 HRV post hoc testing 41
6.3 Anova results of HR(V) during AT 41
6.4 Anova results of MDBF 42
6.5 Anova results of HR(V) during Intervention 43
6.6 Anova results of HR(V) during baseline 46
6.7 Post hoc testing of HR during baseline 46
6.8 Anova results of HR(V) during AT 46
6.9 Anova results of cortisol analysis 48
6.10 Anova results of mood analysis 49

B.1 Anova results of HR(V) between MIST phases 61
B.2 Post hoc testing of HR(V) between MIST phases 62
B.3 Post hoc testing of HR(V) during Intervention 62

Bibliography

[Ame17] American Psychological Association and American Psychological Association. Stress in America: The State of Our Nation. *Stress in America Survey.*, 2017.

[And00] Johan Andersson, Erika Schagatay, Anna Gislén, and Boris Holm. Cardiovascular responses to cold-water immersions of the forearm and face, and their relationship to apnoea. *European journal of applied physiology*, 83(6):566–572, 2000.

[Ben76] T. Bennett, D.J. Hosking, and J.R. Hampton. Cardiovascular reflex responses to apnoeic face immersion and mental stress in diabetic subjects. *Cardiovascular Research*, 10(2):192–199, 1976.

[Ber87] P.V. Bertrand, B.T. Rudd, P.H. Weller, and A.J. Day. Free cortisol and creatinine in urine of healthy children. *Clinical chemistry*, 33(11):2047–2051, 1987.

[Ber97] Gary G. Berntson, J. Thomas Bigger Jr., Dwain L. Eckberg, Paul Grossman, Peter G. Kaufmann, Marek Malik, Haikady N. Nagaraja, Stephen W. Porges, J. Philip Saul, Peter H. Stone, et al. Heart rate variability: origins, methods, and interpretive caveats. *Psychophysiology*, 34(6):623–648, 1997.

[Bre01] Michael Brennan, Marimuthu Palaniswami, and Peter Kamen. Do existing measures of poincare plot geometry reflect nonlinear features of heart rate variability? *IEEE transactions on biomedical engineering*, 48(11):1342–1347, 2001.

[Bro03] Clive M. Brown, Emmanuel O. Sanya, and Max J. Hilz. Effect of cold face stimulation on cerebral blood flow in humans. *Brain research bulletin*, 61(1):81–6, 2003.

[Cac99] John T. Cacioppo, Wendi L. Gardner, and Gary G. Berntson. The affect system has parallel and integrative processing components: Form follows function. *Journal of personality and Social Psychology*, 76(5):839, 1999.

[Cha05] Evangelia Charmandari, Constantine Tsigos, and George Chrousos. Endocrinology of the Stress Response. *Annual Review of Physiology*, 67(1):259–284, 2005.

[Chi09] Alberto Chiesa and Alessandro Serretti. Mindfulness-based stress reduction for stress management in healthy people: a review and meta-analysis. *The journal of alternative and complementary medicine*, 15(5):593–600, 2009.

[Dag09] Alain Dagher, Beth Tannenbaum, Takuya Hayashi, Jens C. Pruessner, and Dharma McBride. An acute psychosocial stress enhances the neural response to smoking cues. *Brain research*, 1293:40–48, 2009.

[Ded05] Katarina Dedovic, Robert Renwick, Najmeh Khalili Mahani, Veronika Engert, Sonia J. Lupien, and Jens C. Pruessner. The Montreal Imaging Stress Task: Using functional imaging to investigate the effects of perceiving and processing psychosocial stress in the human brain. *Journal of Psychiatry and Neuroscience*, 30(5):319–325, 2005.

[Dil16] Alison Dillon, Mark Kelly, Ian H. Robertson, and Deirdre A. Robertson. Smartphone applications utilizing biofeedback can aid stress reduction. *Frontiers in Psychology*, 7(JUN):1–7, 2016.

[DR03] Jane A. Doussard-Roosevelt, Lee Anne Montgomery, and Stephen W. Porges. Short-term stability of physiological measures in kindergarten children: Respiratory sinus arrhythmia, heart period, and cortisol. *Developmental Psychobiology*, 43(3):230–242, 2003.

[Dun07] Adrian J. Dunn. The HPA Axis and the Immune System: A Perspective. *NeuroImmune Biology*, 7:3–15, 2007.

[Eck83] D. L. Eckberg. Human sinus arrhythmia as an index of vagal cardiac outflow. *Journal of Applied Physiology*, 54(4):961–966, 1983.

[Fol10] Paul Foley and Clemens Kirschbaum. Human hypothalamus-pituitary-adrenal axis responses to acute psychosocial stress in laboratory settings. *Neuroscience and Biobehavioral Reviews*, 35(1):91–96, 2010.

[Fre95] Roy Freeman, Richard J. Cohen, and J. Philip Saul. Transfer function analysis of respiratory sinus arrhythmia: a measure of autonomic function in diabetic neuropathy. *Muscle & Nerve: Official Journal of the American Association of Electrodiagnostic Medicine*, 18(1):74–84, 1995.

[Gev14] Nirit Geva, Jens C. Pruessner, and Ruth Defrin. Acute psychosocial stress reduces pain modulation capabilities in healthy men. *PAIN*, 155(11):2418–2425, 2014.

[Goe17] V. C. Goessl, J. E. Curtiss, and S. G. Hofmann. The effect of heart rate variability biofeedback training on stress and anxiety: A meta-analysis. *Psychological Medicine*, 47(15):2578–2586, 2017.

[Goo94] Brett A. Gooden. Mechanism of the human diving response. *Integrative physiological and behavioral science*, 29(1):6–16, 1994.

[Gro90] P. Grossman, J. van Beek, and C. Wientjes. A comparison of three quantification methods for estimation of respiratory sinus arrhythmia. *Psychophysiology*, 27(6):702–14, 1990.

[Gro04] P. Grossman, F. H. Wilhelm, and M. Spoerle. Respiratory sinus arrhythmia, cardiac vagal control, and daily activity. *American Journal of Physiology-Heart and Circulatory Physiology*, 287(2):H728–H734, 2004.

[Gro07] Paul Grossman and Edwin W. Taylor. Toward understanding respiratory sinus arrhythmia: Relations to cardiac vagal tone, evolution and biobehavioral functions. *Biological Psychology*, 74(2):263–285, 2007.

[Ham02] Patrick S. Hamilton. Open source ecg analysis software documentation. *Computers in cardiology*, 2002:101–104, 2002.

[Hau92] M. Hautzinger and M. Bailer. Allgemeine Depressions-Skala [Depression Scale], 1992.

[Hea] Health and Safety Executive, United Kingdom. Health and Safety Statistics. `http://www.hse.gov.uk/statistics/`. Accessed: 13.12.2019.

[Hil17] M. J. Hilz, B. Stemper, P. Sauer, U. Haertl, W. Singer, and F. B. Axelrod. Cold face test demonstrates parasympathetic cardiac dysfunction in familial dysautonomia. *American Journal of Physiology-Regulatory, Integrative and Comparative Physiology*, 276(6):R1833–R1839, 2017.

[Inf] NF2 Information and Inc Services. Trigeminal nerve. `https://www.nf2is.org/cn5.php`. Accessed: 13.12.2019.

[Ing03] Jon T Ingjaldsson, Jon C Laberg, and Julian F Thayer. Reduced heart rate variability in chronic alcohol abuse: relationship with negative mood, chronic thought suppression, and compulsive drinking. *Biological psychiatry*, 54(12):1427–1436, 2003.

[Ior15] Frank Iorfino, Gail A Alvares, Adam J Guastella, and Daniel S Quintana. Cold face test-induced increases in heart rate variability are abolished by engagement in a social cognition task. *Journal of Psychophysiology*, 2015.

[Kat75] Peter G Katona and FELIX Jih. Respiratory sinus arrhythmia: noninvasive measure of parasympathetic cardiac control. *Journal of applied physiology*, 39(5):801–805, 1975.

[Khu06] Ramesh K. Khurana and Roger Wu. The cold face test: A non-baroreflex mediated test of cardiac vagal function. *Clinical Autonomic Research*, 16(3):202–207, 2006.

[Khu07] Ramesh K. Khurana. Cold face test: Adrenergic phase. *Clinical Autonomic Research*, 17(4):211–216, 2007.

[Kim18] Hye-Geum Kim, Eun-Jin Cheon, Dai-Seg Bai, Young Hwan Lee, and Bon-Hoon Koo. Stress and heart rate variability: A meta-analysis and review of the literature. *Psychiatry investigation*, 15(3):235, 2018.

[Kir89] Clemens Kirschbaum and Dirk H. Hellhammer. Salivary cortisol in psychobiological research: an overview. *Neuropsychobiology*, 22(3):150–169, 1989.

[Kir94] Clemens Kirschbaum and Dirk H. Hellhammer. Salivary cortisol in psychoneuroendocrine research: recent developments and applications. *Psychoneuroendocrinology*, 19(4):313–333, 1994.

[Kir95] Clemens Kirschbaum, Karl-Martin Pirke, and Dirk H. Hellhammer. Preliminary evidence for reduced cortisol responsivity to psychological stress in women using oral contraceptive medication. *Psychoneuroendocrinology*, 20(5):509–514, 1995.

[Lag08] Leah Lagos, Evgeny Vaschillo, Bronya Vaschillo, Paul Lehrer, Marsha Bates, and Robert Pandina. Heart Rate Variability Biofeedback as a Strategy for Dealing with Competitive Anxiety : A Case Study. *Biofeedback*, 36(3):109–115, 2008.

[Lan07] Florian Lang and Philipp Lang. *Basiswissen Physiologie*. Springer-Verlag, 2007.

[Led11] Florian Lederbogen, Peter Kirsch, Leila Haddad, Fabian Streit, Heike Tost, Philipp Schuch, Stefan Wüst, Jens C Pruessner, Marcella Rietschel, Michael Deuschle, et al.

City living and urban upbringing affect neural social stress processing in humans. *Nature*, 474(7352):498, 2011.

[Lem11] Jane B. Lemaire, Jean E. Wallace, Adriane M. Lewin, Jill de Grood, and Jeffrey P. Schaefer. The effect of a biofeedback-based stress management tool on physician stress: A randomized controlled clinical trial. *Open Medicine*, 5(4):154–165, 2011.

[Lem15] Frédéric Lemaitre and Bernhard J. Schaller. The Trigeminocardiac Reflex: A Comparison with the Diving Reflex in Humans. *Trigeminocardiac Reflex*, pages 193–206, 2015.

[Mal96] Marek Malik, J Thomas Bigger, A John Camm, Robert E Kleiger, Alberto Malliani, Arthur J Moss, and Peter J Schwartz. Heart rate variability: Standards of measurement, physiological interpretation, and clinical use. *European heart journal*, 17(3):354–381, 1996.

[Mar11] Roberto La Marca, Patricia Waldvogel, Hanna Thörn, Mélanie Tripod, Petra H. Wirtz, Jens C. Pruessner, and Ulrike Ehlert. Association between Cold Face Test-induced vagal inhibition and cortisol response to acute stress. *Psychophysiology*, 48(3):420–429, 2011.

[McE98] Bruce S McEwen. Protective and damaging effects of stress mediators. *New England journal of medicine*, 338(3):171–179, 1998.

[McE00] Bruce S McEwen. Allostasis and allostatic load: implications for neuropsychopharmacology. *Neuropsychopharmacology*, 22(2):108, 2000.

[Mil94] Lyle H Miller, Alma Dell Smith, and Larry Rothstein. *The stress solution: An action plan to manage the stress in your life*. Pocket, 1994.

[Miz12] Romina Mizrahi, Jean Addington, Pablo M Rusjan, Ivonne Suridjan, Alvina Ng, Isabelle Boileau, Jens C Pruessner, Gary Remington, Sylvain Houle, and Alan A Wilson. Increased stress-induced dopamine release in psychosis. *Biological psychiatry*, 71(6):561–567, 2012.

[Mou04] Laurent Mourot, Malika Bouhaddi, Stéphane Perrey, Sylvie Cappelle, Marie-Thérèse Henriet, Jean-Pierre Wolf, Jean-Denis Rouillon, and Jacques Regnard. Decrease in heart rate variability with overtraining: assessment by the poincare plot analysis. *Clinical physiology and functional imaging*, 24(1):10–18, 2004.

[Nat09] Urs M. Nater and Nicolas Rohleder. Salivary alpha-amylase as a non-invasive biomarker for the sympathetic nervous system: Current state of research. *Psychoneuroendocrinology*, 34(4):486–496, 2009.

[Nel80] Erland Nelson, J. R. Hebel, Ramesh K. Khurana, Sadakiyo Watabiki, and Rodrigo Toro. Cold face test in the assessment of trigeminal-brainstem- vagal function in humans. *Annals of Neurology*, 7(2):144–149, 1980.

[Orb13] Sheina Orbell, Havah Schneider, and Sabrina Esbitt. Hypothalamic-Pituitary-Adrenal Axis. In *Encyclopedia of Behavioral Medicine*, pages 1017–1018. Springer New York, New York, NY, 2013.

[Pri11] Gabriell E. Prinsloo, H.G. Laurie Rauch, Michael I. Lambert, Frederick Muench, Timothy D. Noakes, and Wayne E. Derman. The effect of short duration heart rate variability (hrv) biofeedback on cognitive performance during laboratory induced cognitive stress. *Applied Cognitive Psychology*, 25(5):792–801, 2011.

[Pru03] Jens C. Pruessner, Clemens Kirschbaum, Gunther Meinlschmid, and Dirk H. Hellhammer. Two formulas for computation of the area under the curve represent measures of total hormone concentration versus time-dependent change. *Psychoneuroendocrinology*, 28(7):916–931, 2003.

[Pru08] Jens C Pruessner, Katarina Dedovic, Najmeh Khalili-Mahani, Veronika Engert, Marita Pruessner, Claudia Buss, Robert Renwick, Alain Dagher, Michael J Meaney, and Sonia Lupien. Deactivation of the limbic system during acute psychosocial stress: evidence from positron emission tomography and functional magnetic resonance imaging studies. *Biological psychiatry*, 63(2):234–240, 2008.

[Rai07] Rainforth MV, Schneider RH, Nidich SI, Gaylord-King C, Salerno JW, and Anderson JW. Stress reduction programs in patients with elevated blood pressure: a systematic review and meta-analysis. *Current Hypertension Reports*, 9(6):520–8, 2007.

[Ric15] Robert Richer, Tim Maiwald, Cristian Pasluosta, Bernhard Hensel, and Bjoern M Eskofier. Novel human computer interaction principles for cardiac feedback using google glass and android wear. In *2015 IEEE 12th International Conference on Wearable and Implantable Body Sensor Networks (BSN)*, pages 1–6. IEEE, 2015.

[Sam14] S Sammito, B Thielmann, R Seibt, A Klussmann, M Weippert, and I Böckelmann. S2k-Leitlinie: Nutzung der Herzschlagfrequenz und der Herzfrequenzvariabilität in

der Arbeitsmedizin und der Arbeitswissenschaft. *AWMF online - Das Portal der wissenschaftlichen Medizin*, 11(11):1–60, 2014.

[Sat09] Maharana Satyapriya, Hongasanda R. Nagendra, Raghuram Nagarathna, and Venkatram Padmalatha. Effect of integrated yoga on stress and heart rate variability in pregnant women. *International Journal of Gynecology and Obstetrics*, 104(3):218–222, 2009.

[Sch96] Erika Schagatay and Boris Holm. Effects of water and ambient air temperatures on human diving bradycardia. *European journal of applied physiology and occupational physiology*, 73(1-2):1–6, 1996.

[Sch10] Alice Schmidt, Erich Möstl, Christiane Wehnert, Jörg Aurich, Jürgen Müller, and Christine Aurich. Cortisol release and heart rate variability in horses during road transport. *Hormones and Behavior*, 57(2):209–215, 2010.

[Sch13] Robert F. Schmidt and Gerhard Thews. *Physiologie des Menschen*. Springer-Verlag, 2013.

[Sgo15] Andrea Sgoifo, Luca Carnevali, Maria De Los Angeles Pico Alfonso, and Mario Amore. Autonomic dysfunction and heart rate variability in depression. *Stress*, 18(3):343–352, 2015.

[Ski11] Martie L. Skinner, Elizabeth A. Shirtcliff, Kevin P. Haggerty, Christopher L. Coe, and Richard F. Catalano. Allostasis model facilitates understanding race differences in the diurnal cortisol rhythm. *Development and psychopathology*, 23(4):1167–1186, 2011.

[Sol11] Alexandra Soliman, Gillian A O'Driscoll, Jens Pruessner, Ridha Joober, Blaine Ditto, Elizabeth Streicker, Yael Goldberg, Josie Caro, P Vivien Rekkas, and Alain Dagher. Limbic response to psychosocial stress in schizotypy: a functional magnetic resonance imaging study. *Schizophrenia Research*, 131(1-3):184–191, 2011.

[Ste97] Rolf Steyer, Peter Schwenkmezger, Peter Notz, and Michael Eid. Der mehrdimensionale befindlichkeitsfragebogen MDBF [multidimensional mood questionnaire]. *Göttingen, Germany: Hogrefe*, 1997.

[Ste16] Mary Ann C. Stephens, Pamela B. Mahon, Mary E. McCaul, and Gary S. Wand. Hypothalamic–pituitary–adrenal axis response to acute psychosocial stress: effects of biological sex and circulating sex hormones. *Psychoneuroendocrinology*, 66:47–55, 2016.

[Tha06a] Julian F. Thayer, Martica Hall, John J. Sollers, and Joachim E. Fischer. Alcohol use, urinary cortisol, and heart rate variability in apparently healthy men: Evidence for impaired inhibitory control of the HPA axis in heavy drinkers. *International Journal of Psychophysiology*, 59(3):244–250, 2006.

[Tha06b] Julian F. Thayer and Esther Sternberg. Beyond heart rate variability: Vagal regulation of allostatic systems. *Annals of the New York Academy of Sciences*, 1088:361–372, 2006.

[Tha07] Julian F. Thayer and Richard D. Lane. The role of vagal function in the risk for cardiovascular disease and mortality. *Biological Psychology*, 74(2):224–242, 2007.

[Tha12] Julian F. Thayer, Fredrik Åhs, Mats Fredrikson, John J. Sollers, and Tor D. Wager. A meta-analysis of heart rate variability and neuroimaging studies: Implications for heart rate variability as a marker of stress and health. *Neuroscience and Biobehavioral Reviews*, 36(2):747–756, 2012.

[Tul96] Mikko P. Tulppo, T.H. Makikallio, T.E. Takala, T.H.H.V. Seppanen, and Heikki V. Huikuri. Quantitative beat-to-beat analysis of heart rate dynamics during exercise. *American journal of physiology-heart and circulatory physiology*, 271(1):H244–H252, 1996.

[vdZ15] Judith Esi van der Zwan, Wieke de Vente, Anja C. Huizink, Susan M. Bögels, and Esther I. de Bruin. Physical Activity, Mindfulness Meditation, or Heart Rate Variability Biofeedback for Stress Reduction: A Randomized Controlled Trial. *Applied Psychophysiology Biofeedback*, 40(4):257–268, 2015.

[Wec09] Jill M. Wecht, Joseph P. Weir, Ronald E. Demeersman, Gregory J. Schilero, John P. Handrakis, Michael F. Lafountaine, Christopher M. Cirnigliaro, Steven C. Kirshblum, and William A. Bauman. Cold face test in persons with spinal cord injury: Age versus inactivity. *Clinical Autonomic Research*, 19(4):221–229, 2009.

[Wei03] Bryan J. Weiner and Eric M. Zimmerman. Blood Pressure and Emotional Health. *The Journal of Alternative and Complementary Medicine*, 9(3):355–369, 2003.

[Zuc09] Terri L. Zucker, Kristin W. Samuelson, Frederick Muench, Melanie A. Greenberg, and Richard N. Gevirtz. The effects of respiratory sinus arrhythmia biofeedback on heart rate variability and posttraumatic stress disorder symptoms: A pilot study. *Applied Psychophysiology Biofeedback*, 34(2):135–143, 2009.